

NASA TECHNICAL NOTE



NASA TN D-3066

c. 1

LOAN COPY: RETL  
AFWL (WLIL-1)  
KIRTLAND AFB, N

0130109



TECH LIBRARY KAFB, NM

NASA TN D-3066

# VIBRATION TESTS OF PRESSURIZED THIN-WALLED CYLINDRICAL SHELLS

*by Robert Miserentino and Louis F. Vosteen*

*Langley Research Center*

*Langley Station, Hampton, Va.*



NATIONAL AERONAUTICS AND SPACE ADMINISTRATION • WASHINGTON, D. C. • OCTOBER 1965



0130109

NASA TN D-3066

VIBRATION TESTS OF PRESSURIZED THIN-WALLED  
CYLINDRICAL SHELLS

By Robert Miserentino and Louis F. Vosteen

Langley Research Center  
Langley Station, Hampton, Va.

NATIONAL AERONAUTICS AND SPACE ADMINISTRATION

---

For sale by the Clearinghouse for Federal Scientific and Technical Information  
Springfield, Virginia 22151 - Price \$2.00

# VIBRATION TESTS OF PRESSURIZED THIN-WALLED CYLINDRICAL SHELLS

By Robert Miserentino and Louis F. Vosteen  
Langley Research Center

## SUMMARY

The breathing vibration modes of seven unstiffened cylinders having radius-to-thickness ratios ranging from 324 to 1622 have been determined. Six cylinders were made of stainless steel and one, of aluminum. Their nominal length-to-radius ratio was six. Experimental results are presented to show the variations of resonant frequency and mode shape with internal pressure. The experimental results compared favorably with Reissner's analysis based upon Donnell's equation. However, the theory tended to overestimate the frequency increase which resulted from an increase in internal pressure.

## INTRODUCTION

Pressurized thin-walled unstiffened circular cylinders are presently being used as propellant tanks and primary structures for launch vehicles and spacecraft. Consequently, their response to the dynamic loads associated with the launch environment is of prime importance to the designer. The solution to dynamic loading problems is dependent on accurate methods for predicting the natural vibration modes and frequencies.

As part of a study to determine the dynamic behavior of thin-walled cylinders, the natural vibration modes and frequencies of seven unstiffened cylinders subjected to internal pressure and various longitudinal loads have been experimentally determined. The radius-to-thickness ratios of these cylinders ranged from 324 to 1624. Six cylinders were made of stainless steel and one, of aluminum. Their nominal length-to-radius ratio was six. The vibration frequencies measured were for the shell breathing modes in which the axis of the cylinder remained undeformed, and the elements of the wall performed harmonic motions predominately in the radial direction. The experimental results were then compared with the results obtained from Donnell's equation (ref. 1), sometimes referred to as Reissner's shallow-shell theory (ref. 2).

## SYMBOLS

The units used for the physical quantities in this paper are given both in the U.S. Customary Units and in the International System of Units (SI). Factors relating the two systems are given in reference 3 and those used in the present investigation are presented in the appendix.

A	ratio of the area that produces a pressure-dependent axial load to the total circular cross-sectional area
a	mean radius of cylinder, in. (m)
c	edge fixity constant ( $c = 0$ for simply supported cylinder)
E	Young's modulus, lb/in <sup>2</sup> (N/m <sup>2</sup> )
f	frequency, cps (Hz)
h	skin thickness, in. (m)
k	frequency parameter, $\frac{\rho}{E}(2\pi fa)^2$
k <sub>0</sub>	frequency parameter at zero internal pressure
l	free length of cylinder in the longitudinal direction, in. (m)
m	number of half-waves in the longitudinal direction
n	number of full waves in the circumferential direction
n <sub>x</sub>	nondimensional axial tension due to external load, $\frac{N_x}{Eh}$
$\bar{n}_x$	nondimensional axial tension due to internal pressure, $\frac{N_x}{Eh}$
$\bar{n}_\phi$	nondimensional circumferential tension due to internal pressure, $\frac{\bar{N}_\phi}{Eh}$
N <sub>x</sub>	axial load per unit length due to external load, lb/in. (N/m)
$\bar{N}_x$	axial load per unit length due to internal pressure, $A \frac{pa}{2}$ , lb/in. (N/m)
$\bar{N}_\phi$	circumferential load per unit length due to internal pressure, pa, lb/in. (N/m)

p	internal pressure, psi ( $\text{N/m}^2$ )
$\lambda$	axial wavelength parameter, $\frac{\pi a}{l}(m + c)$
$\mu$	Poisson's ratio
$\rho$	mass density, $\text{lb-sec}^2/\text{in}^4$ ( $\text{kg/m}^3$ )

## MODELS, APPARATUS, AND TESTS

### Cylinder Models

A total of seven cylinders was constructed; six, of stainless steel and one, of aluminum. Five cylinders had a nominal radius of 6 inches (15 cm) and two had a radius of 4 inches (10 cm). The nominal radius-to-thickness ratios were from 324 to 1624. These ratios are the basis for the reference numbers for each cylinder. Construction details of the cylinders are shown in figure 1, and photographs in figure 2. The photographs, however, are not representative of the condition of the cylinders during vibration tests since they were taken after buckling tests (not reported herein) had been performed. The physical properties and dimensions of each cylinder are given in table I.

Steel end-rings were bonded with an epoxy adhesive to facilitate handling and attachment to the test fixture. In all cases the various end-rings provided essentially clamped supports.

Cylinders 324, 601, 1001, and 1502 had end-rings that were attached to the support fixture with screws through radial holes. This method caused distortion of the cylinder and made it difficult to obtain a tight seal. The other cylinders were mounted with screws extending longitudinally through holes in the end-rings. (See figs. 1(b) and 1(c).)

### Test Apparatus

Fixtures.- All cylinders were mounted on support fixtures that were fundamentally the same. The fixtures consisted of a thick-walled cylindrical support affixed to a heavy mounting base (figs. 3 and 4). The support fits inside the cylinder and the aft end-ring of the cylinder is clamped to an attachment-ring while the forward end of the cylinder is closed with a heavy bulkhead. Some details of this design resulted from aerodynamic considerations which are not reported herein.

For the present vibration tests, the only difference in fixtures or end-rings which could affect the results involves the attachment-ring near the base. The cylinders with a 6-inch (15-cm) radius were attached, as shown in figures 3(a) and 3(b), directly to a heavy ring with a T-shaped cross section. The ring moved on three O rings that sealed the cylinder chamber. The T-ring

provided a means of applying an axial tensile or compressive load to the cylinder. The cylinders with a 4-inch (10-cm) radius (fig. 3(c)) were attached to a heavy ring that was centered on the central shaft by a thin guiding plate. The ring in turn could be attached to a heavy T-ring through four axial bolts instrumented for measuring axial loads. The chamber was sealed by a flexible rubberized fabric membrane as shown in figure 3(c). The method of attachment for the cylinders with the 6-inch (15-cm) radius would be expected to approximate more nearly a fixed-end condition than that of the cylinders with the 4-inch (10-cm) radius.

Cylinder pressurizing system.- A pressure-regulating system supplied by a compressed-air source was used to pressurize the cylinders. A Bourdon tube pressure gage was used to measure the internal pressure. The gage and the regulator were tapped into opposite ends of the chamber formed by the cylinder and fixture. A calibration test showed the gage to be accurate within one-half of 1 percent of the scale value, and zero shifts during a test were less than one division of the gage, 0.005 psi ( $34 \text{ N/m}^2$ ).

Vibration equipment.- An electromechanically modulated air-powered loud speaker was used to excite harmonic vibrations of the cylinders. (See fig. 5.) This type of vibration exciter has the advantage of not applying a concentrated force or adding an appreciable mass to the thin walls of the cylinders. The measured acoustic pressure at the test cylinder was 113 dB with a flatness tolerance of 15 dB in the frequency range of 60 to 1000 cps (Hz).

Variations in deflection around the circumference were measured with a variable-reluctance pickup at a point  $2/5$  the length of the cylinder from the aft end. The variable-reluctance pickup was chosen because it does not contact the model. The pickup was rotated around the cylinder on a motor-driven ring at the rate of 1 rpm. The pickup was automatically positioned radially to the desired distance from the cylinder wall by a servosystem. Thus any variations in circularity or misalignment of the pickup support did not affect the amplitude of the ac signal produced by the vibrating cylinder. Longitudinal variations in the response deflections were measured by either a line of 12 internally mounted reluctance pickups or a hand-held velocity probe with a spring constant of 9 grams force per inch ( $3.4 \text{ N/m}$ ).

The ac output of one pickup at a time was displayed along with the shaker oscillator signal on an oscilloscope. The frequency of the pickup signal was read on a frequency meter with an accuracy of 0.5 percent.

### Test Procedure

Data were obtained by setting either the chamber pressure or the frequency and varying the other until a peak amplitude response (which was taken to be the resonant point) was seen on the oscilloscope. With both the frequency and pressure held at this resonant point, the pickup was driven around the cylinder to determine the location and number of circumferential half-waves. The mode was identified by a double index -  $n$  for the number of waves around the circumference and  $m$  for the number of half-waves in the longitudinal direction.

Other observations, such as the relative magnitude of the resonant peak, position of node lines with respect to the welds, spacing of node lines, and phase relations were recorded to help to correlate the data.

In order to minimize the locally induced stresses due to misalignment of the end-rings, the attachments were tightened while the cylinder was vibrating in a low-frequency mode. If the frequency was observed to shift as the bolts were tightened, the attachment was realigned until the effect was minimized.

Since the response of a mode is influenced by the orientation of the exciting force field, the loud speaker was moved often to reduce the possibility of modes being overlooked. When it was difficult to pick out a resonance peak, the pickup position, as well as the frequency and the pressure, was varied.

## RESULTS AND DISCUSSION

The measured pressures and resonant frequencies for all recorded modes are tabulated in table II for each test cylinder. Also noted in table II are instances when the node lines regularly assumed a particular orientation with respect to the longitudinal seams. In addition, data for a mechanically applied axial load are presented in table III for cylinders 324 and 666.

In table III the loads are given in nondimensional form. It should be pointed out that throughout the text  $n_x$  is the nondimensional axial tension load due to external loads only and  $\bar{n}_x$  is the nondimensional axial tension load due to internal pressure only, and that  $\bar{n}_x = \frac{A}{2} \frac{pa}{Eh}$ . Where A for the cylinders with a 6-inch (15-cm) radius was 0.2336 and for the cylinders with a 4-inch (10-cm) radius was 0.3237.

### Results for Cylinder With $\frac{a}{h} = 324$

The test results in table II for cylinder 324, which is the one with the smallest value of  $a/h$ , are summarized in figure 6. The square of the natural frequency is plotted as a function of internal pressure for modes with one half-wave in the longitudinal direction ( $m = 1$ ) and for a range of circumferential nodes ( $n = 2$  to 9). Solid straight lines representing a "least-squares" fit through the data points are also shown. The frequency-pressure relation represented by these lines can be expressed in general as  $f^2 = c_1 + c_2 p$  which is nondimensionalized to the form

$$k = k_0 + \frac{dk}{d\bar{n}_\phi} \bar{n}_\phi \quad (1)$$

where

$$k_0 = 4\pi^2 a^2 \frac{\rho}{E} c_1$$

$$\frac{dk}{d\bar{n}_\phi} = 4\pi^2 a h \rho c_2$$

and

$$\bar{n}_\phi = \frac{pa}{Eh}$$

where  $c_1$  and  $c_2$  are constants determined from the experimental data. From this definition of  $k$  (eq. (1)) it follows that  $k_0$  is the nondimensional frequency of the unpressurized cylinder.

Similar conclusions were arrived at theoretically by Reissner in reference 2 where it is shown that values of  $k_0$  and  $\frac{dk}{d\bar{n}_\phi}$  can be written as

$$k_0 = \frac{\lambda^4}{(n^2 + \lambda^2)^2} + \frac{(h/a)^2}{12(1 - \mu^2)}(n^2 + \lambda^2)^2 + n_x \lambda^2 \quad (2)$$

and

$$\frac{dk}{d\bar{n}_\phi} = \lambda^2 \frac{d\bar{n}_x}{d\bar{n}_\phi} + n^2$$

For the cylinders reported herein,  $\frac{dk}{d\bar{n}_\phi}$  can be expressed as

$$\frac{dk}{d\bar{n}_\phi} = \frac{A}{2} \lambda^2 + n^2 \quad (3)$$

where  $A$  accounts for the pressure acting on the attachment-ring, seals, and membrane. The definition of the axial wavelength parameter  $\lambda = \frac{\pi a}{l}(m + c)$  is based on reference 4 where it is suggested that the coefficient  $c$  be added to  $m$  to account for the effective change in length of a simply supported cylinder due to the clamping action on the ends. A value of  $c = 0.3$  was found in reference 4 to correlate theoretical results for clamped and simply supported cylinders.

A comparison between the theoretical and experimental frequency is shown in figure 7. The results are plotted in terms of the nondimensional frequency  $k$  and the nondimensional pressure parameter  $\bar{n}_\phi$ . From the figure it can be seen that, with the exception of  $n = 2$ , which is a predominantly bending mode, the agreement between theory and experiment is good. Even for the  $n = 2$  case the slopes  $\frac{dk}{d\bar{n}_\phi}$  of the lines are approximately the same; the difference is in the value of the intercept  $k_0$ .

The difference between theory and experiment is more easily seen in figures 8 and 9. In figure 8 both the theoretical and the experimental values of  $k_0$  are plotted as a function of the mode number  $n$ . The experimental values in



figure 8 are the intercepts of the "least-square" lines in figure 7 and represent the frequency of the cylinder with no pressure.

In figure 9, the experimental and theoretical values of  $\frac{dk}{d\bar{n}_\phi}$  are presented as a function of mode number  $n$ . Note that the theoretical contribution to a change in frequency by the axial stress due to pressure (the first term in equation (3)) is negligible for  $m = 1$  compared with the contribution of circumferential stress; thus,  $\frac{dk}{d\bar{n}_\phi} \approx n^2$ . From figure 9 it can be seen that except for the case where  $n = 2$ , the experimentally determined slopes are slightly lower than those calculated theoretically. Differences range from 6 to 15 percent for the modes measured.

#### Results for Cylinder With Various Values of $a/h$

The effects of increasing the  $a/h$  ratio on the accuracy of theoretically predicted frequency can be seen in figures 10 and 11. In figure 10 the experimental results of  $k_0$  as a function of  $n$  are compared with the theoretical results for cylinders with  $a/h$  values from 601 to 1624. Although the trends of the experiment and theory agree, a comparison of these results shows that, for modes with  $n$  near that of the lowest frequency mode, cylinders with small  $a/h$  ratios show a much closer agreement than do cylinders of  $a/h$  greater than a 1000. Also note that with the exception of  $n = 2$  and  $n = 3$  the experimental values of  $k_0$  were higher than the calculated ones. Good comparison between theory and experiment for  $n = 2$  or  $n = 3$ , however, should not be expected as the Donnell equations, used in the derivation, are applicable only for larger values of  $n$ .

Figure 11 indicates that the increase in frequency due to an increase in internal pressure  $\frac{dk}{d\bar{n}_\phi}$  is always overestimated by theory. The percentage difference between theoretical and experimental values of  $\frac{dk}{d\bar{n}_\phi}$  are fairly uniform for each cylinder. However, there is a slight tendency for the percent difference first to increase and then decrease as  $n$  is increased, as is the case for the cylinders tested in reference 5 ( $a/h = 937$  and  $3000$ ).

Most of the irregularity in the deviation of the data from the trends shown by the theory can be attributed to an insufficient number of points to average out measuring errors or imperfections in the cylinder. Although no measurements were made of deviations from circularity or variations in skin thickness, visual inspection suggests a ranking (in order of least deviation) of 324, 645, 601, 1624, 666, 1502, and 1001.

From figures 8 to 11, it can be concluded that there is good agreement between theoretical and experimental frequencies for the minimum frequency modes in a range of small values of the pressure parameter  $\bar{n}_\phi$  from  $0.15 \times 10^{-5}$  to  $10.00 \times 10^{-5}$ . Beyond this range the larger theoretical slope  $\frac{dk}{d\bar{n}_\phi}$  results in increased separation between theory and experiment. (See eq. (1).)

## Results for Modes With $m > 1$

Within the frequency range of the investigation many circumferential modes with more than one longitudinal half-wave ( $m > 1$ ) were observed. These modes, however, were often dominated by the nearness of similar modes with one longitudinal half-wave and were therefore difficult to isolate. The greatest number of such modes (with  $m > 1$ ) were observed and recorded for cylinder 645. The results of these observations are shown in figure 12, where  $k_0$  is plotted as a function of  $n$  for the modes with  $m = 1, 2$ , and  $3$ . In addition, the corresponding theoretical values, as obtained from equation (2), are shown in the figure. The experimental results agree relatively well with theory for  $m = 2$ , but for  $m = 3$  the experimental values of  $k_0$  are considerably lower than those obtained theoretically. Similar results were obtained for all other cylinders tested except for cylinder 1001, which had substantially more imperfections than the other cylinders. In this case, poor agreement between theory and experiment was found even for the  $m = 2$  results. In all cylinders the experimental values of  $\frac{dk}{dn_\phi}$  for  $m > 1$  were similar to those for  $m = 1$ .

## Results for Applied Longitudinal Load

In an effort to obtain the influence of longitudinal load on the frequencies of cylinders, two of the cylinders were subjected to longitudinal loads. The results of these tests are shown in figures 13 and 14. In figure 13, the frequency parameter  $k_0$  is plotted against the mechanically applied axial tension load ( $n_x$ ) for zero internal pressure for cylinder 324. It can be seen that except for  $n = 2$ , the axial stresses have no appreciable effect on the frequency. This conclusion is in agreement with the theoretical results shown in equation (2).

Similar results were observed for cylinder 666 (fig. 14) when one resonant mode was followed through elastic compression into the buckling load region. In order to stabilize the shape of the cylinder an internal pressure was maintained.

## Experimental Observations

The experimental program involved determining modes and frequencies for different loads at over 1000 data points. Most of the modal shapes investigated had some pressure range where their resonant peak and associated mode shape could be accurately observed. Consequently, in these pressure ranges experimental scatter was small. However, identification of the natural mode was difficult for certain pressure ranges. These difficulties could be attributed to a variety of causes. For example, in certain pressure ranges, several modes occur in a narrow frequency bandwidth and, theoretically, could have the same frequency. In these cases neither mode could be observed accurately.

Another important factor causing experimental scatter is the imperfections existing in the cylinders. The effects of general shell imperfections in the experimentally obtained slope (shown in fig. 11) have already been discussed.

Other types of imperfections such as asymmetry in the cylinder and overlapping of the skin at seam joints also contributed to the experimental uncertainties. In all cases an increase in internal pressure tended to decrease the scattering of data points due to imperfections.

As shown in reference 6, slight asymmetries in a cylinder may resolve a given natural mode of a perfect cylinder into two modes of similar shape but slightly different natural frequencies. This effect has been observed in other investigations (for example, ref. 7) and was encountered in the present tests as shown in figure 10(b) for cylinder 645. In this case the imperfections caused by welded seams caused a regular separation of some modes into two different orientations, one positioned so that a node line runs through each welded seam.

Another factor of some interest is the effect of the bolted attachment of the end-rings of the cylinders. To partially evaluate the importance of this attachment, tests were run on cylinder 324 with the attachment bolts removed from the aft end-ring. The cylinder was mounted vertically. The observed new natural frequencies of the modes are shown in figure 15 along with the theoretical curves obtained for a fixity coefficient  $c$  of 0.3 and 0. It can be seen that, by freeing one end of the cylinder, the measured frequencies for the small values of  $n$  are considerably reduced and higher values of  $n$  may be increased by a slight amount. For modes with  $n$  near that of the minimum frequency mode, very little effect was observed.

The exact resonant frequency was sometimes obscured by the fact that the amplitude of vibration did not peak at any distinct frequency, but remained fairly constant over a wide frequency bandwidth. Difficulties also arose when trying to determine a resonant mode shape accurately. In these instances a large amplitude was seen over a substantial region of the cylinder with no apparent node lines; it thus became necessary to count the amplitude peaks. A similar phenomenon was observed in reference 5 and was attributed to waves traveling around the cylindrical circumference. This behavior occurred most often in the cylinders with higher  $a/h$  values and sometimes in a wide frequency bandwidth that often included more than one resonant frequency.

A slight nonlinearity in the response of the most responsive modes was seen at times. The peak resonant amplitude was greater and at a higher frequency if the shaker frequency was increased to the resonant frequency than if it were decreased through the same resonant mode.

#### CONCLUDING REMARKS

The natural modes and frequencies of seven thin-walled circular cylinders were determined experimentally for various values of internal pressure and end loads. The cylinders had a length-to-radius ratio of six and the radius-to-thickness ratios varied from 324 to 1622. A small internal pressure caused a significant increase in resonant frequency over that for zero pressure as well as a reduction in experimental scatter which seemed to be associated with initial imperfections. Changes in end load (tension or compression) caused very little change in frequency over the elastic range covered in this investigation.

Comparison of the experimental results with Donnel shallow-shell theory showed reasonably good agreement except for the mode involving two waves in the circumferential direction. However, the theory tends to overestimate the resonant frequency increase which occurred in this experiment due to an increase in internal pressure.

Langley Research Center,  
National Aeronautics and Space Administration,  
Langley Station, Hampton, Va., June 4, 1965.

## APPENDIX

### CONVERSION OF U.S. CUSTOMARY UNITS TO SI UNITS

Factors for converting U.S. Customary Units to the International System of Units (SI) are given in the following table:

Physical quantity	U.S. Customary Unit	Conversion factor (*)	SI unit
Axial load	lb/in.	175.1	newtons/meter (N/m)
Frequency	cps	1	hertz (Hz)
Length	in.	0.0254	meters (m)
Mass density	lb-sec <sup>2</sup> /in <sup>4</sup>	703.07	kilograms/meter <sup>3</sup> (kg/m <sup>3</sup> )
Pressure	psi	$6.895 \times 10^3$	newtons/meter <sup>2</sup> (N/m <sup>2</sup> )
Radius	in.	0.0254	meters (m)
Thickness	in.	0.0254	meters (m)
Young's modulus	lb/in <sup>2</sup>	$6.895 \times 10^3$	newtons/meter <sup>2</sup> (N/m <sup>2</sup> )

\*Multiply value given in U.S. Customary Unit by conversion factor to obtain equivalent value in SI unit.

Prefixes to indicate multiples of units are as follows:

Prefix	Multiple
giga (G)	$10^9$
kilo (k)	$10^3$
centi (c)	$10^{-2}$
milli (m)	$10^{-3}$

## REFERENCES

1. Donnel, L. H.: Stability of Thin-Walled Tubes Under Torsion. NACA Rept. 479, 1933.
2. Reissner, Eric: Non-Linear Effects in Vibrations of Cylindrical Shells. Rept. No. AM 5-6, Guided Missile Res. Div., The Ramo-Wooldridge Corp., Sept. 30, 1955.
3. Mechtly, E. A.: The International System of Units - Physical Constants and Conversion Factors. NASA SP-7012, 1964.
4. Arnold, R. A.; and Warburton, G. B.: The Flexural Vibrations of Thin Cylinders. Proc. (A) Inst. of Mech Engrs. (London), vol. 167, no. 1, 1953, pp. 62-74.
5. Mixon, John S.; and Herr, Robert W.: An Investigation of the Vibration Characteristics of Pressurized Thin-Walled Circular Cylinders Partially Filled With Liquid. NASA TR R-145, 1962.
6. Tobias, S. A.: A Theory of Imperfection for the Vibration of Elastic Bodies of Revolution. Engineering, vol. 172, no. 4470, Sept. 28, 1951, pp. 409-410.
7. Fung, Y. C.; Sechler, E. E.; and Kaplan, A.: On the Vibration of Thin Cylindrical Shells Under Internal Pressure. Aero. Sci., vol. 24, no. 9, 1957, pp. 650-660.

TABLE I.- PHYSICAL PROPERTIES OF CYLINDERS

a			l		h		Material	ρ		E		μ Number of seam welds	
a/h								lb-s <sup>2</sup> /in <sup>4</sup>	kg/m <sup>3</sup>	psi	GN/m <sup>2</sup>		
	in.	m	in.	m	in.	mm							
324	6.01	15.27	36.00	91.44	0.0185	0.4699	17-7 PH stainless steel	0.7149 × 10 <sup>-3</sup>	7639	29.0 × 10 <sup>6</sup>	200	0.28	2
601	6.01	15.27	36.00	91.44	.0100	.2540	301 stainless steel	.7408	7916	29.0	200	.32	2
645	4.00	10.16	24.00	60.96	.0062	.1575	301 stainless steel	.7408	7916	29.0	200	.32	2
666	4.00	10.16	24.00	60.96	.0060	.1524	301 stainless steel	.7408	7916	29.0	200	.32	2
1001	6.01	15.27	36.00	91.44	.0060	.1524	2024 aluminum	.2524	2699	10.0	72.3	.32	4
1502	6.01	15.27	36.00	91.44	.0040	.1016	304 stainless steel	.7408	7916	29.0	200	.32	1
1624	6.01	15.27	38.20	97.03	.0037	.0940	301 stainless steel	.7408	7916	29.0	200	.32	2

TABLE II.- MEASURED MODES, RESONANT FREQUENCIES, AND PRESSURES FOR ALL CYLINDERS

Cylinder	m	n	f cps or Hz	p		Cylinder	m	n	f cps or Hz	p		Cylinder	m	n	f cps or Hz	p	
				psi	kN/m <sup>2</sup>					psi	kN/m <sup>2</sup>					psi	kN/m <sup>2</sup>
324	1	a <sub>2</sub>	387	0	0	601	1	3	252	0	0	601	1	10	585	5.00	34.47
		a <sub>2</sub>	391	2.00	13.78				259	1.00	6.89				673	7.00	48.26
		b <sub>2</sub>	398	6.00	41.36				269	2.00	13.78				744	9.00	62.05
		b <sub>2</sub>	400	8.00	55.15				280	4.00	27.57				781	10.00	68.94
		a <sub>2</sub>	396	8.00	55.15				297	7.00	48.26						
		b <sub>2</sub>	403	9.00	62.05				312	9.00	62.05						
		a <sub>2</sub>	402	10.00	68.94				313	10.00	68.94						
								4	165	0	0		645	1	11	338	0
									190	1.00	6.89				12	453	2.00
									207	2.00	13.78						
									241	4.00	27.57						
									255	5.00	34.47						
									283	7.00	48.26						
	3								307	9.00	62.05						
									319	10.00	68.94						
								5	122	0	0						
									169	1.00	6.89						
									201	2.00	13.78						
									256	4.00	27.57						
	4								276	5.00	34.47						
									323	7.00	48.26						
									355	9.00	62.05						
									373	10.00	68.94						
	5							6	121	0	0						
									180	1.00	6.89						
									226	2.00	13.78						
									296	4.00	27.57						
									328	5.00	34.47						
									377	7.00	48.26						
	6								425	9.00	62.05						
									446	10.00	68.94						
	7							7	270	2.00	13.78						
									349	4.00	27.57						
									447	7.00	48.26						
									500	9.00	62.05						
									524	10.00	68.94						
	8							8	315	2.00	13.78						
									410	4.00	27.57						
									450	5.00	34.47						
									519	7.00	48.26						
									581	9.00	62.05						
	9							9	222	0	0						
									303	1.00	6.89						
									365	2.00	13.78						
									463	4.00	27.57						
									502	5.00	34.47						
									592	7.00	48.26						
601	1	2	381	0	0		10	420	420	2.00	13.78		645	a <sub>7</sub>	415	2.06	14.20
			392	1.00	6.89				540	4.00	27.57				523	3.62	24.96
			394	4.00	27.57										587	4.69	32.34
			395	5.00	34.47										659	6.18	42.61
			399	7.00	48.26												
			397	9.00	52.05												
			398	10.00	68.94												
								420									

<sup>a</sup>Node lines are on seam welds.<sup>b</sup>Node lines are off seam welds.



TABLE II.- MEASURED MODES, RESONANT FREQUENCIES, AND PRESSURES FOR ALL CYLINDERS - Continued

Cylinder	m	n	f cps or Hz	P		Cylinder	m	n	f cps or Hz	P		Cylinder	m	n	f cps or Hz	P			
				psi	kN/m <sup>2</sup>					psi	kN/m <sup>2</sup>					psi	kN/m <sup>2</sup>		
645	1	a7	698	7.05	48.61	645	1	12	740	1.16	7.99	666	1	b2	659	0	0		
			740	7.95	34.13				784	1.56	10.76				671	4.05	27.92		
			784	9.01	62.12				988	3.66	25.24				669	6.20	42.75		
			830	10.20	70.33										671	6.60	45.51		
			b8	329	0.55			3.79	2	6	523				3.81	26.27	672	6.90	47.58
		466		2.03	13.99			587			5.49				37.85	673	8.00	55.15	
		587		3.51	24.20			659			7.38				50.88	675	8.10	55.85	
		659		4.55	31.37			830			12.85				88.60	677	8.30	57.23	
		698		5.16	35.58											675	8.70	59.99	
		740		5.91	40.75			7		415	1.46				10.07	674	8.90	61.36	
		784		6.78	46.75					659	5.60				38.61	670	9.50	65.50	
		830		7.73	52.98					698	6.54				45.09	672	10.00	68.94	
		988		11.20	77.22					740	7.50				51.71	674	10.20	70.33	
										784	8.61				59.36	679	11.10	76.53	
										830	9.86				67.98	680	12.40	85.50	
		a8	466	1.76	12.13			8	587	3.08	21.24			3	415	2.00	13.78		
			587	3.32	22.89					4.71	32.47				435	3.20	22.06		
			784	6.57	45.30					5.51	37.99				439	3.30	22.75		
			830	7.46	51.44					6.31	43.51				437	3.40	23.44		
			988	11.08	76.40					7.28	50.19				447	4.30	29.65		
		b9	329	0.15	1.03				9	587	1.99				13.72	447	4.40	30.34	
			415	.67	4.62					659	2.91				20.06	448	4.50	31.03	
			466	1.07	7.38					698	3.36				23.17	451	4.80	33.09	
			587	2.29	15.79					740	4.01				27.65	458	5.10	35.16	
			659	3.17	21.86					784	4.57				31.51	457	5.40	37.23	
			698	3.74	25.79			10		988	7.88				54.33	462	6.00	41.36	
			740	4.30	29.65											463	6.10	42.06	
			784	4.94	34.06					587	1.32				9.10	473	6.55	45.16	
			830	5.66	39.03					659	1.99				13.72	472	6.80	46.89	
			988	8.44	58.19					698	2.40				16.55	472	6.90	47.58	
	a9		415	0.59	4.07		3	6	740	2.85	19.65		476		7.30	50.33			
			698	3.65	25.17				988	6.06	41.78		479		7.60	52.40			
			740	4.17	28.75								486		8.00	55.15			
			784	4.81	33.16								484		8.10	55.85			
			830	5.51	37.99								484		8.10	55.85			
			988	8.15	56.19				523	3.34	23.03		491		8.30	57.23			
	b10		415	0.37	2.55			7	587	5.00	34.48		490		8.70	59.86			
			466	.75	5.17				659	6.84	47.16		490		8.78	60.54			
			659	2.30	15.86				698	8.09	55.78		490		8.80	60.68			
			784	3.69	25.44				740	9.31	64.19		492		8.90	61.37			
			932	5.53	38.13				932	12.35	85.15		494		9.00	62.06			
	a10		466	0.45	3.10			8	587	3.92	27.03		494		9.00	62.06			
			587	1.45	9.99				659	5.35	36.89		496		9.30	64.12			
			659	2.11	14.55				698	6.24	43.02		500		9.60	66.19			
			698	2.56	17.65				740	7.16	49.36		506		10.20	70.33			
			740	2.98	20.55				784	8.17	56.33		513		11.10	76.53			
	11		784	3.41	23.51			9	830	9.36	64.54		513		11.28	77.78			
			988	6.19	42.68								522		12.40	78.60			
									740	5.35	36.89		4	367	4.20	28.96			
									784	6.12	42.19			373	4.30	29.65			
									830	7.12	49.09			383	4.30	29.65			
														394	4.79	33.03			
														441	6.80	46.89			
														446	7.65	52.75			
														464	7.90	54.47			
														485	8.10	55.85			
														525	11.10	76.53			

<sup>a</sup>Node lines are on seam welds.<sup>b</sup>Node lines are off seam welds.

TABLE II.- MEASURED MODES, RESONANT FREQUENCIES, AND PRESSURES FOR ALL CYLINDERS - Continued

Cylinder	m	n	f cps or Hz	P		Cylinder	m	n	f cps or Hz	P		Cylinder	m	n	f cps or Hz	P						
				psi	kN/m <sup>2</sup>					psi	kN/m <sup>2</sup>					psi	kN/m <sup>2</sup>					
666	1	5	402	4.30	29.65	666	1	6	703	10.90	75.16	666	1	9	1045	9.00	62.01					
			424	4.70	32.41				714	10.90	75.16				10	405	0	0				
			418	4.75	32.75				7	579	4.00					27.57	543	1.00	6.89			
			466	5.75	39.65					597	4.40					30.34	569	1.35	9.31			
			492	6.80	46.89					639	5.30					36.54	591	1.35	9.31			
			519	7.40	51.02					648	5.40					37.23	671	2.00	13.78			
			508	7.40	51.02					656	5.60					38.61	731	2.90	19.99			
			507	7.40	51.02					659	5.70					39.30	741	2.90	19.99			
			513	7.60	52.40					677	5.95					41.03	800	3.35	23.10			
			523	7.60	52.40					673	6.00					41.36	835	4.00	27.57			
			524	7.95	54.82					690	6.35					43.78	890	4.75	32.75			
			529	8.00	55.16					697	6.45					44.47	910	5.20	35.85			
			529	8.10	55.85					701	6.60					45.51	910	5.20	35.85			
			527	8.10	55.85					709	6.70					46.20	934	5.50	37.92			
			536	8.10	55.85					713	6.80					46.89	978	5.80	39.99			
			548	8.50	58.61					736	7.40					51.02	1029	6.70	46.20			
			544	8.70	59.99					761	8.00					55.15	1179	9.00	62.06			
			556	8.70	59.99					761	8.00					55.15	1188	9.10	62.75			
			549	9.00	62.55					766	8.20					56.54	11	149	0	0		
			552	9.10	62.75					768	8.20					56.54		598	1.00	6.89		
			578	9.50	65.50					794	8.70					59.99		622	1.00	6.89		
			567	9.70	66.88					821	9.50					65.50		751	2.00	13.78		
			590	10.10	69.64					818	9.50					65.50		798	2.25	15.51		
			651	12.40	85.49					826	9.60					66.19		800	2.27	15.65		
			651	12.75	87.91					826	9.80					67.57		850	3.25	22.41		
	6	6	402	3.00	20.68			8	449	1.35	9.31					897	3.30	22.75				
			412	3.20	22.06				568	2.90	19.99				903	3.40	23.44					
			415	3.25	22.41				580	3.00	20.69				962	4.00	27.57					
			437	3.60	24.82				631	3.90	26.89				970	4.10	28.27					
			458	4.00	27.57				663	4.30	29.65				1120	6.45	44.47					
			471	4.30	29.65				684	4.80	33.10			12	732	1.00	6.89					
			493	4.80	33.10				749	5.70	39.30				800	1.65	11.38					
			498	5.00	34.47				755	6.00	41.36				850	2.00	13.79					
			505	5.20	35.86				777	6.60	45.51				883	2.25	15.51					
			515	5.30	36.54				781	6.60	45.51				946	2.90	19.99					
			517	5.40	37.23				781	6.70	46.20				1054	4.10	28.27					
			531	5.70	39.30				850	7.95	54.82				1247	6.45	44.47					
			531	5.75	39.65				848	8.10	55.85			13	800	0.65	4.48					
			548	6.20	42.75				883	8.70	59.98				814	.80	5.52					
			556	6.45	44.47				888	8.90	61.37				850	1.10	7.58					
			573	6.70	46.19				884	9.00	62.06				991	2.25	15.51					
			578	6.90	47.57				922	9.60	66.19				1182	4.10	28.70					
			580	7.10	48.95				915	9.60	66.19				14	1077	2.25	15.51				
			596	7.40	51.02				937	10.00	68.94					1140	2.90	19.99				
			600	7.60	52.40				9	537	1.35					9.31	1253	4.10	28.27			
			615	7.90	54.47					648	2.90					19.99	1520	6.90	47.58			
			620	8.00	55.15					671	2.90					19.99	15	1029	0.70	4.83		
			619	8.00	55.15					719	3.60					24.82		1628	6.00	41.36		
			621	8.10	55.85					758	3.90					26.89		16	1105	0.70	4.83	
			616	8.10	55.85					759	4.10					28.27			18	1425	0.70	4.83
			631	8.30	57.22					804	4.75					32.75						
			629	8.50	58.61					902	6.40					44.13						
			639	8.70	59.99					927	7.00					48.26						
			635	8.78	60.54																	
			645	9.10	62.75																	
			675	10.00	68.94																	
			685	10.00	68.94																	

TABLE II.-- MEASURED MODES, RESONANT FREQUENCIES, AND PRESSURES FOR ALL CYLINDERS - Continued

Cylinder	m	n	f cps or Hz	P		Cylinder	m	n	f cps or Hz	P		Cylinder	m	n	f cps or Hz	P			
				psi	kN/m <sup>2</sup>					psi	kN/m <sup>2</sup>					psi	kN/m <sup>2</sup>		
666	2	3	967	3.30	22.75	666	2	5	678	9.25	63.77	1001	1	8	821	6.00	41.36		
			964	3.40	23.44				680	9.25	63.77				9	408	1.00	6.89	
			970	4.10	28.27				684	9.50	65.50					729	4.00	27.57	
			970	4.75	32.75				683	9.60	66.18					10	474	1.00	6.89
			978	5.40	37.23				684	9.60	66.18				610		2.00	13.78	
			978	5.80	39.99				693	10.00	68.94				816		4.00	27.57	
			973	6.30	43.44				696	10.20	70.32			11	545	1.00	6.89		
			982	6.35	43.78				714	10.90	75.15				717	2.00	13.78		
			982	6.50	44.81				723	11.10	76.53				850	3.00	20.68		
			980	6.60	45.51			6	497	3.40	23.44			12	617	1.00	6.89		
			979	6.90	47.58				524	3.90	26.88				784	2.00	13.78		
			982	7.00	48.27				545	4.30	29.64				951	3.00	20.68		
			983	7.00	48.27				544	4.40	30.33				1190	5.00	34.47		
			990	8.00	55.15				591	5.25	36.19		13	657	1.00	6.89			
			991	8.10	55.85				607	5.70	39.30			1303	5.00	34.47			
			986	8.20	56.54				609	6.00	41.36		14	699	1.00	6.89			
			992	8.85	61.02				624	6.20	42.74			940	2.00	13.78			
			991	8.90	61.37				630	6.45	44.47			1260	4.00	27.57			
			990	9.00	62.06				646	6.90	47.57			1300	5.00	34.47			
	997	9.60	66.19	1001	1	2	262	1.00	6.89	15	798			1.00	6.89				
	997	9.60	66.19				276	2.00	13.78		1019			2.00	13.78				
	995	9.80	67.57				297	4.00	27.57		1568			5.00	34.47				
	993	9.90	68.26				317	6.00	41.36	16	938			1.00	6.89				
	1002	10.00	68.95				262	2.00	13.78		1169			2.00	13.78				
	1054	11.11	76.60				280	3.00	20.68		1685			5.00	34.47				
	4		666				3.00	20.69	3	262	2.00			13.78	2	276	2.00	13.78	
			670			3.40	23.44	280		3.00	20.68			316		4.00	27.57		
			682			3.50	24.13	297		4.00	27.57			336		5.00	34.47		
			677			4.30	29.65	313		5.00	34.47			354	6.00	41.36			
			699			4.75	32.75	4	212	1.00	6.89			4	238	1.00	6.89		
			716			6.00	41.36		276	2.00	13.78				375	4.00	27.57		
			715			6.30	43.44		322	3.00	20.68				423	5.00	34.47		
			723			6.42	44.27		401	5.00	34.47			5	231	1.00	6.89		
			716			6.70	46.20	430	6.00	41.36	315				2.00	13.78			
			725			6.95	47.92	5	225	1.00	6.89				371	3.00	20.68		
			739			8.10	55.85		301	2.00	13.78				426	4.00	27.57		
			743			8.15	56.19		356	3.00	20.68			473	5.00	34.47			
			758			9.33	64.33		413	4.00	27.57			514	6.00	41.36			
			764			9.80	67.57	7	453	5.00	34.47			6	287	1.00	6.89		
			765			10.00	68.94		494	6.00	41.36				520	4.00	27.57		
			778			11.10	76.53		8	283	1.00			6.89	576	5.00	34.47		
			790			12.40	85.50	365		2.00	13.78			7	330	1.00	6.89		
			5				537	3.30		22.75	443				3.00	20.68	432	2.00	13.78
							545	3.65		25.17	507				4.00	27.57	528	3.00	20.68
							556	3.90		26.89	517				6.00	41.36	613	4.00	27.57
							554	4.00		27.57									
							579	4.00		27.57									
							570	4.30		29.65									
							581	4.80		33.20									
	579	4.80					33.09												
	585	5.00					34.47												
	617	5.95					41.02												
	630	6.90					47.57												
	652	8.00					55.15												
	645	8.10					55.84												
	676	9.00					62.05												

TABLE II.- MEASURED MODES, RESONANT FREQUENCIES, AND PRESSURES FOR ALL CYLINDERS - Continued

Cylinder	m	n	f cps or Hz	P		Cylinder	m	n	f cps or Hz	P		Cylinder	m	n	f cps or Hz	P								
				psi	kN/m <sup>2</sup>					psi	kN/m <sup>2</sup>					psi	kN/m <sup>2</sup>							
1001	2	7	683	5.00	34.47	1502	2	7	550	5.00	34.47	1624	1	4	446	10.00	68.94							
		8	373 608 764	1.00 3.00 5.00	6.89 20.68 34.47			10	506	2.00	13.78			466 481 494 514	11.00 12.00 13.00 14.00	75.84 82.73 89.63 96.52								
1502	1	2	451 452 459 461	2.00 3.00 4.00 5.00	13.78 20.68 27.57 34.47	1624	1	2	424 419 416 432 420 433 426 429 448 430 434 432 432 433 444 435 432 421	1.00 2.00 3.00 4.00 5.00 6.00 7.00 8.00 9.00 10.00 11.00 11.00 12.00 13.00 14.00	6.89 13.78 20.68 27.57 27.57 34.47 34.47 41.36 47.57 48.26 55.15 62.05 68.94 75.84 75.84 82.73 89.63 96.52	5		126 203 266 281 318 323 349 370 397 405 429 463 472 504 521 505 521 532 547 558 571 586 594 609 613 627 665 639	0 1.00 2.00 2.30 3.00 3.00 3.50 4.00 4.00 5.00 5.00 6.00 6.00 7.00 7.00 8.00 9.00 9.00 10.00 10.00 11.00 11.00 12.00 12.00 13.00 13.00 14.00 14.00	0 6.89 13.78 15.85 20.68 20.68 24.13 27.57 27.57 34.47 34.47 41.36 41.36 48.26 48.26 55.15 62.05 62.05 68.94 68.94 75.84 75.84 82.73 82.73 89.63 89.63 96.52 96.52								

TABLE II.- MEASURED MODES, RESONANT FREQUENCIES, AND PRESSURES FOR ALL CYLINDERS - Concluded

Cylinder	m	n	f cps or Hz	P		Cylinder	m	n	f cps or Hz	P		
				psi	kN/m <sup>2</sup>					psi	kN/m <sup>2</sup>	
1624	1	7	316	1.46	10.06	1624	1	9	261	0.55	3.79	
			364	2.00	13.78				344	1.00	6.89	
			382	2.2	15.16				413	1.53	10.54	
			441	3.00	20.68				472	2.03	13.99	
			479	3.5	24.13				569	3.00	20.68	
			497	4.00	27.57				682	4.40	30.33	
			524	4.4	30.33				717	5.00	34.47	
			551	5.00	34.47				793	6.00	41.36	
			558	5.00	34.37				813	6.30	43.43	
			606	6.00	41.36				971	9.00	62.05	
			617	6.00	41.36				1017	10.00	68.94	
			634	6.3	43.43				1068	11.00	75.84	
			652	7.00	48.26			10	237	0.25	1.72	
			740	9.00	62.05				294	.55	3.79	
			775	10.00	68.94				389	1.00	6.89	
			814	11.00	75.84				458	1.47	10.13	
			820	11.00	75.84				530	2.00	13.78	
			881	13.00	89.63				529	2.02	13.92	
		8	231	0.55	3.79				569	2.38	16.40	
			289	1.00	6.89				632	3.00	20.68	
			358	1.47	10.13				631	3.00	20.68	
			412	1.94	13.37				696	3.50	24.13	
			419	2.00	13.78				772	4.44	30.61	
			437	2.20	15.16			11	323	0.55	3.79	
			468	2.56	17.65				410	1.00	6.89	
			501	3.00	20.68				763	3.50	24.13	
			502	3.00	20.68				848	4.40	30.33	
			510	3.00	20.68				1293	11.00	75.84	
			539	3.50	24.13		12		208	0	0	
			564	4.00	27.57				1004	6.20	42.74	
			579	4.00	27.57				1077	7.00	48.26	
			633	5.00	34.47				1223	9.00	62.05	
			642	5.00	34.47				1350	11.00	75.84	
			671	5.46	37.64		2	3	672	9.00	62.05	
			696	6.00	41.36				4	473	11.00	75.84
			709	6.10	42.05					529	11.00	75.84
			751	7.00	48.26			8		1183	14.00	96.52
			807	8.00	55.15							
			847	9.00	62.05							
			892	10.00	68.94							
			943	11.00	75.84							
			1022	13.00	89.63							

TABLE III.- MEASURED FREQUENCIES AND MODES FOR MECHANICALLY APPLIED AXIAL LOADS  
FOR CYLINDERS 324 AND 666

(a) Cylinder 324

m	n	Frequency, f, cps (or Hz) for -				
		$\bar{n}_x=0$ $n_x=0.3827 \times 10^{-3}$ $\bar{n}_\phi=0$	$\bar{n}_x=0$ $n_x=0.1275 \times 10^{-3}$ $\bar{n}_\phi=0$	$\bar{n}_x=0$ $n_x=0.2551 \times 10^{-3}$ $\bar{n}_\phi=0$	$\bar{n}_x=0.0231 \times 10^{-6}$ $n_x=0.2551 \times 10^{-3}$ $\bar{n}_\phi=0.1974 \times 10^{-6}$	$\bar{n}_x=0.0576 \times 10^{-6}$ $n_x=0.2551 \times 10^{-3}$ $\bar{n}_\phi=0.4936 \times 10^{-6}$
1	2	---	329	399	---	407
	3	254	250	252	262	281
	4	177	172	175	216	266
	5	167	162	165	231	303
	6	196	191	194	276	364
	7	247	243	246	346	---
	8	323	320	321	415	527
2	5	303	291	294	337	400

m	n	f, * cps (or Hz) for $\bar{n}_x=n_x=\bar{n}_\phi=0$
1	a <sub>2</sub>	337
	a <sub>3</sub>	228
	a <sub>4</sub>	168
	a <sub>5</sub>	160
	a <sub>6</sub>	190
	a <sub>7</sub>	244
	a <sub>8</sub>	317
	a <sub>9</sub>	399
2	5	284
3	b <sub>7</sub>	251

\* Aft ring disconnected from fixture.

<sup>a</sup>Node lines are on seam welds.

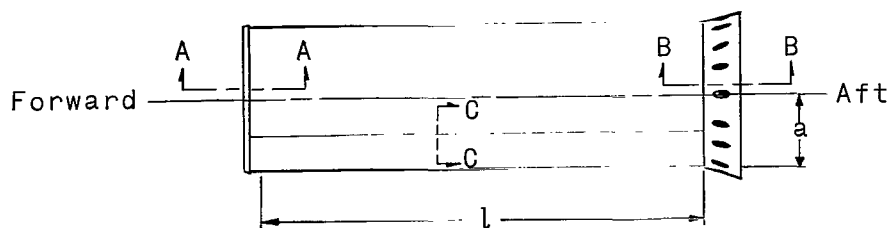
<sup>b</sup>Node lines are off seam welds.

TABLE III.- MEASURED FREQUENCIES AND MODES FOR MECHANICALLY APPLIED AXIAL LOADS  
FOR CYLINDERS 324 AND 666 - Concluded

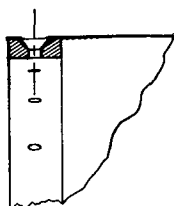
(b) Cylinder 666 with  $m = 1$  and  $n = 3$

$\bar{n}_x$	$\bar{n}_\phi$	Frequency, $f$ , cps (or Hz) for $n_x = 0.8559 \times 10^{-3}$
$0.248 \times 10^{-6}$	$1.532 \times 10^{-6}$	470
.296	1.829	485
.307	1.898	492
.407	2.515	526

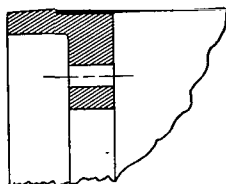
$\bar{n}_x$	Frequency, $f$ , cps (or Hz) for $\bar{n}_x = 0.299 \times 10^{-6}$ and $\bar{n}_\phi = 1.852 \times 10^{-6}$
0	484
$-0.8559 \times 10^{-3}$	481
-1.1984	480
-1.7120	468
-1.8833	466
-2.2599	452
- - - - - Buckle - - - - -	
-2.4312	438
-2.6365	344
- - - - - Collapse - - - - -	



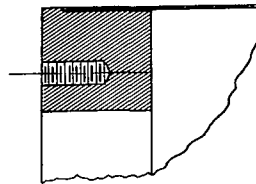
(a) Overall view of typical cylinder.



For cylinders  
324, 601, 1001, and 1502

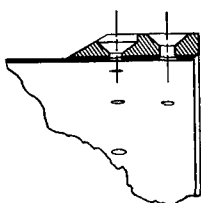


For cylinder 1624

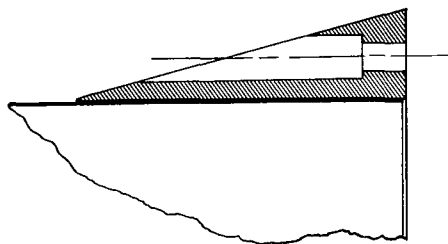


For cylinders  
645 and 666

(b) Cross-sectional view of forward end-rings. Section AA of figure 1(a).



For cylinders 324, 601,  
1001, and 1502



For cylinders 1624,  
645, and 666

(c) Cross-sectional view of aft end-rings. Section BB of figure 1(a).



For cylinders 324, 601,  
1001, 1502, and 1624  
3 rows of spotwelds,  
1/8 inch (0.32 cm)  
between spots



For cylinders 645 and 666  
2 seamwelds

(d) Sketch of the 1/2-inch (1.27-cm) overlap used in the longitudinal seam joints. Section CC of figure 1(a).

Figure 1.- Details of cylinder.





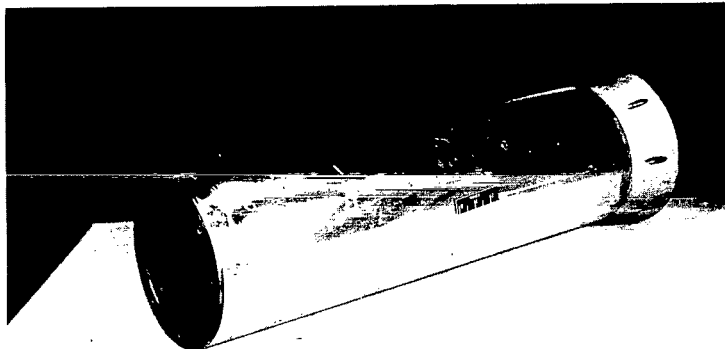
(a) Cylinder 1001.

L-62-8992



(b) Cylinder 1624.

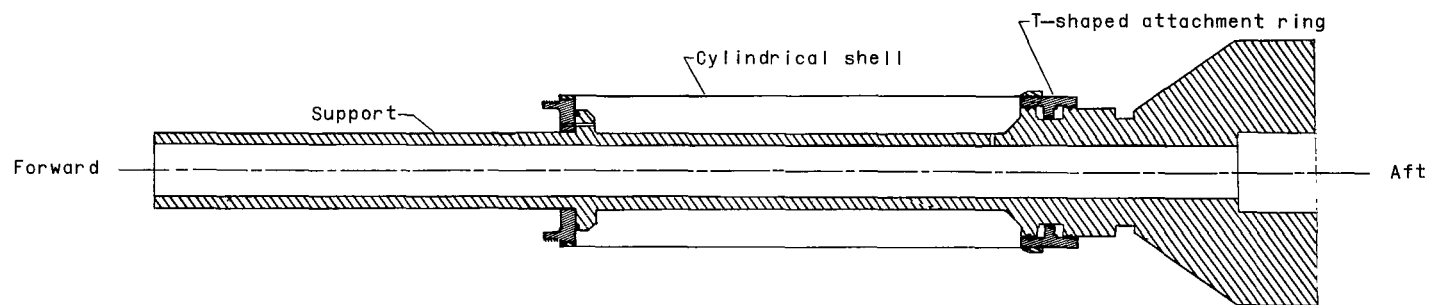
L-62-8989



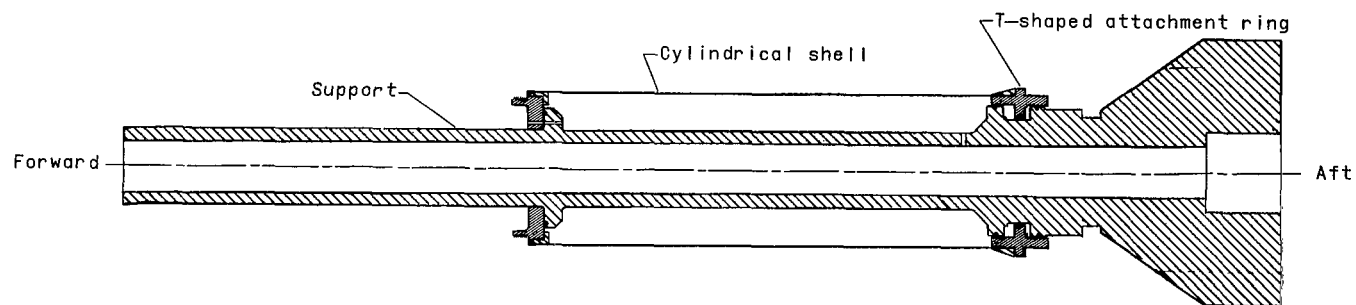
(c) Cylinder 645.

L-62-8988

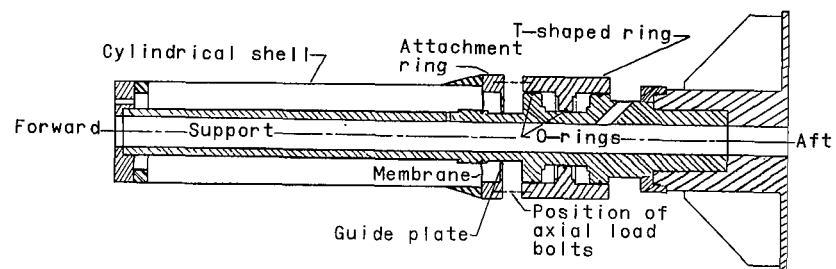
Figure 2.- Photographs of cylinders.



(a) Cylinder with 6-inch (15-cm) radius bolted radially to fixture.

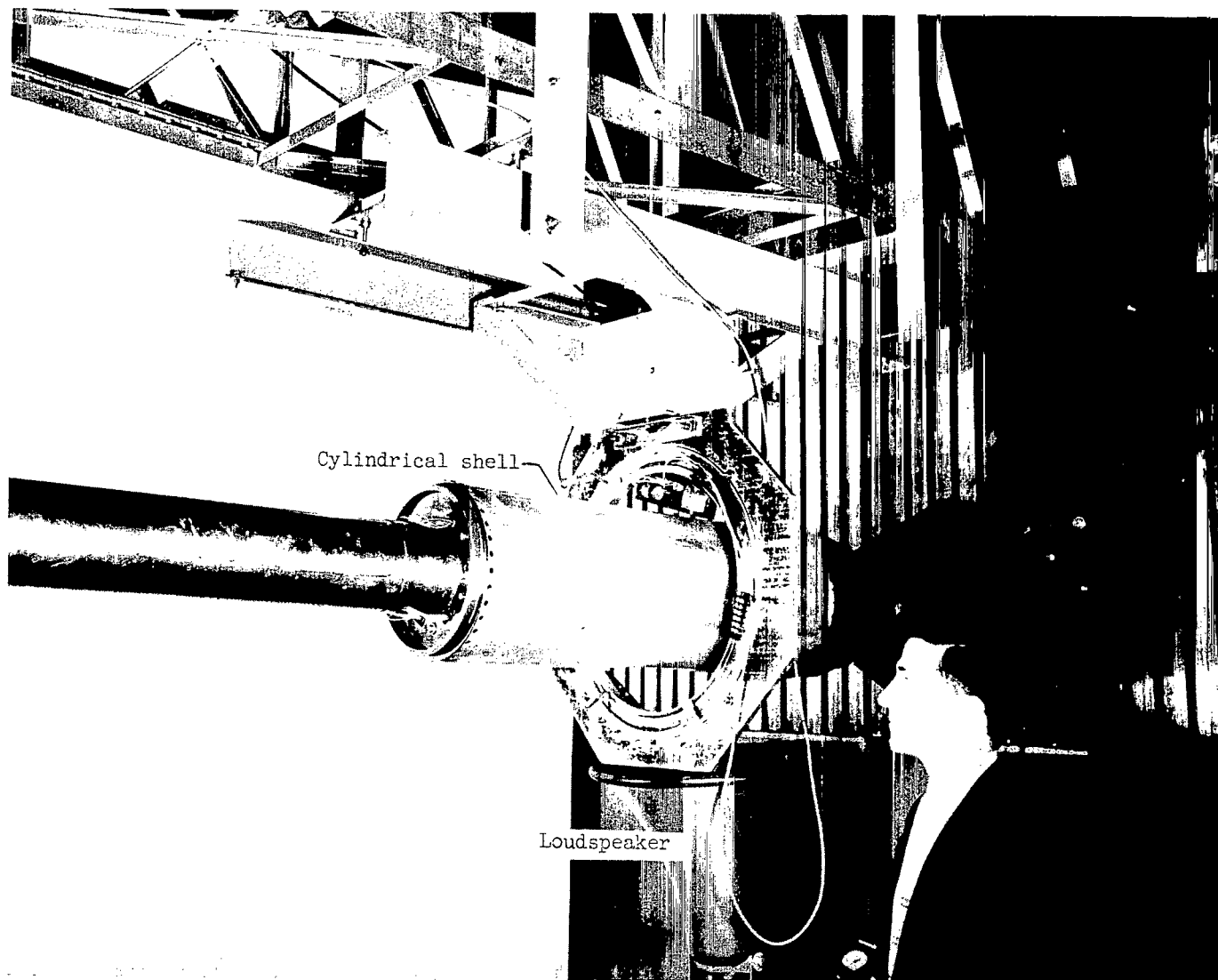


(b) Cylinder with 6-inch (15-cm) radius bolted longitudinally to fixture.



(c) Cylinder with 4-inch (10-cm) radius in place on fixture.

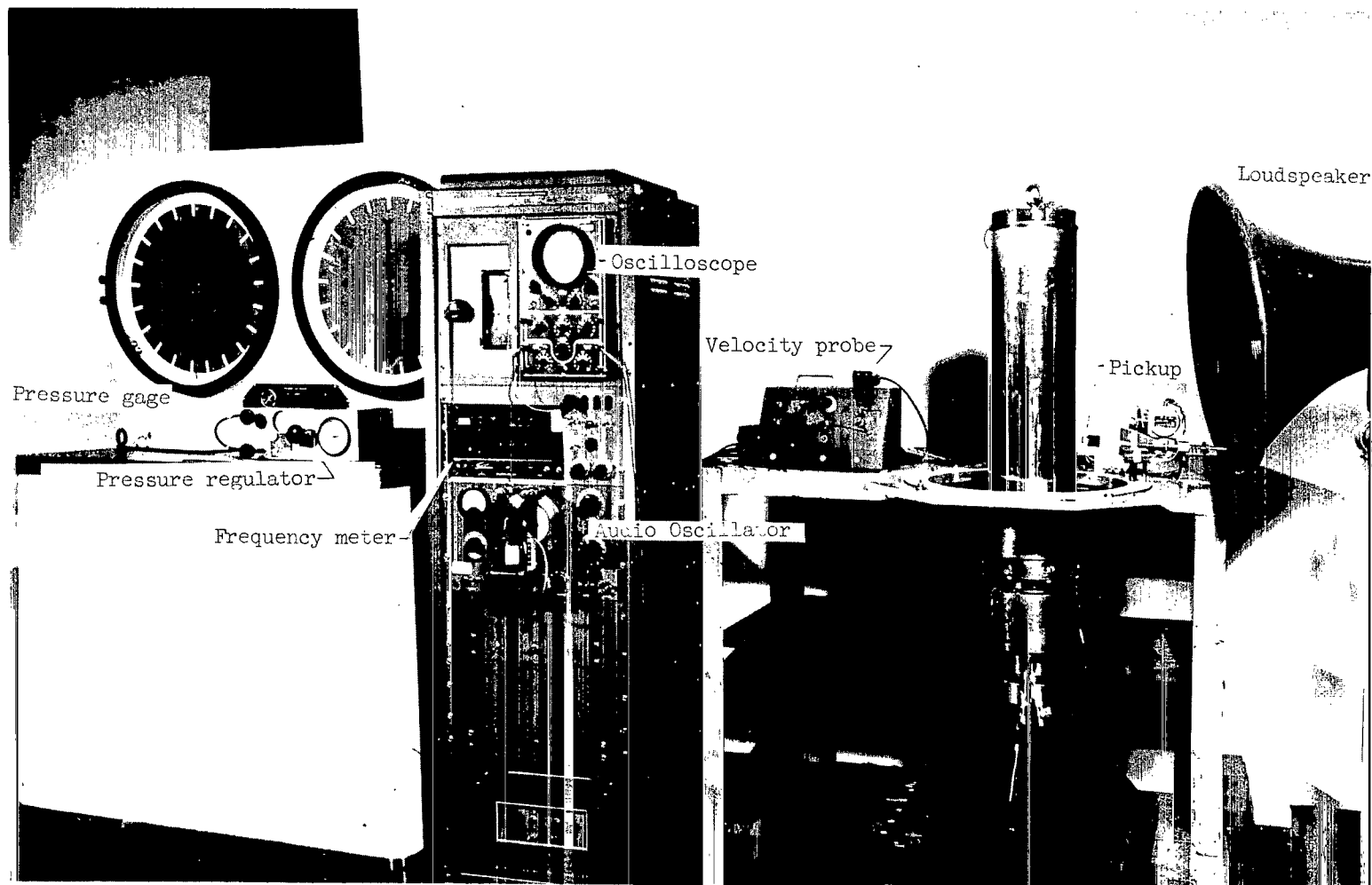
Figure 3.- Cross sections of cylinders.



(a) Horizontal setup for cylinders with 6-inch (15-cm) radius.

L-59-7777.1

Figure 4.- Photographs of test setups.



(b) Test equipment and vertical model setup.

L-62-8994.1

Figure 4.- Concluded.

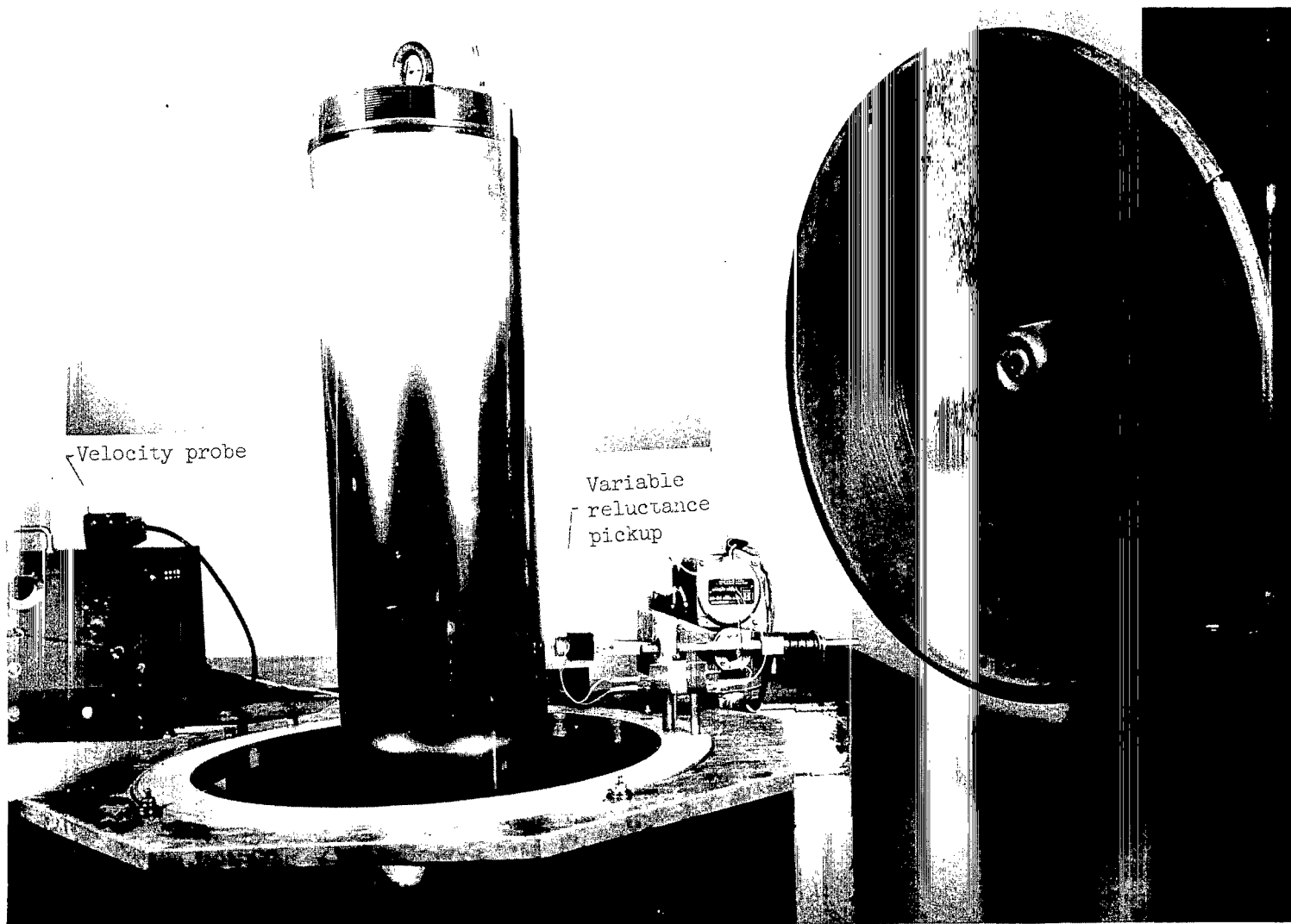


Figure 5.- Photograph of pickup.

L-62-8993.1

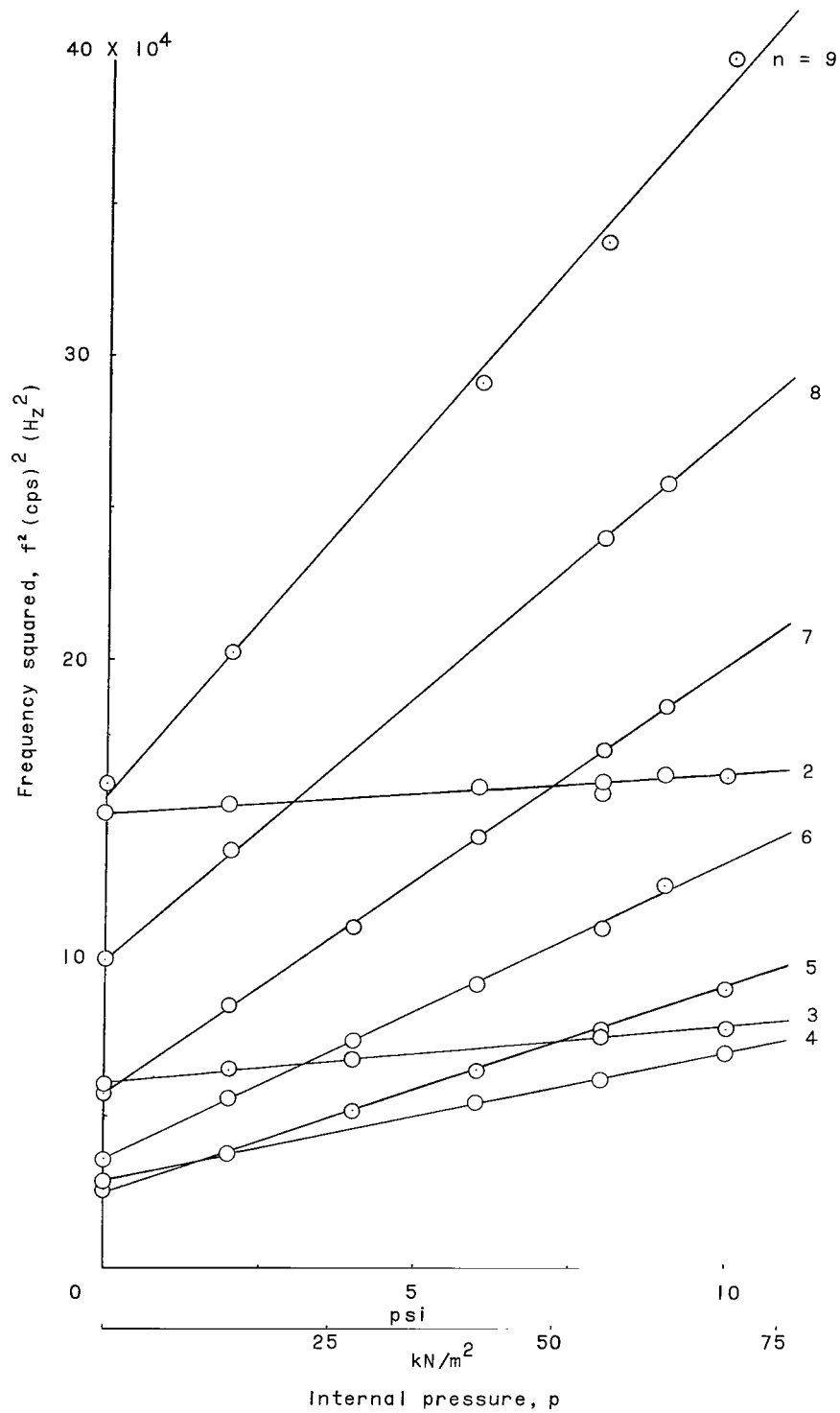


Figure 6.- Experimental variation of squared frequency with pressure for cylinder 324 with no external axial load.

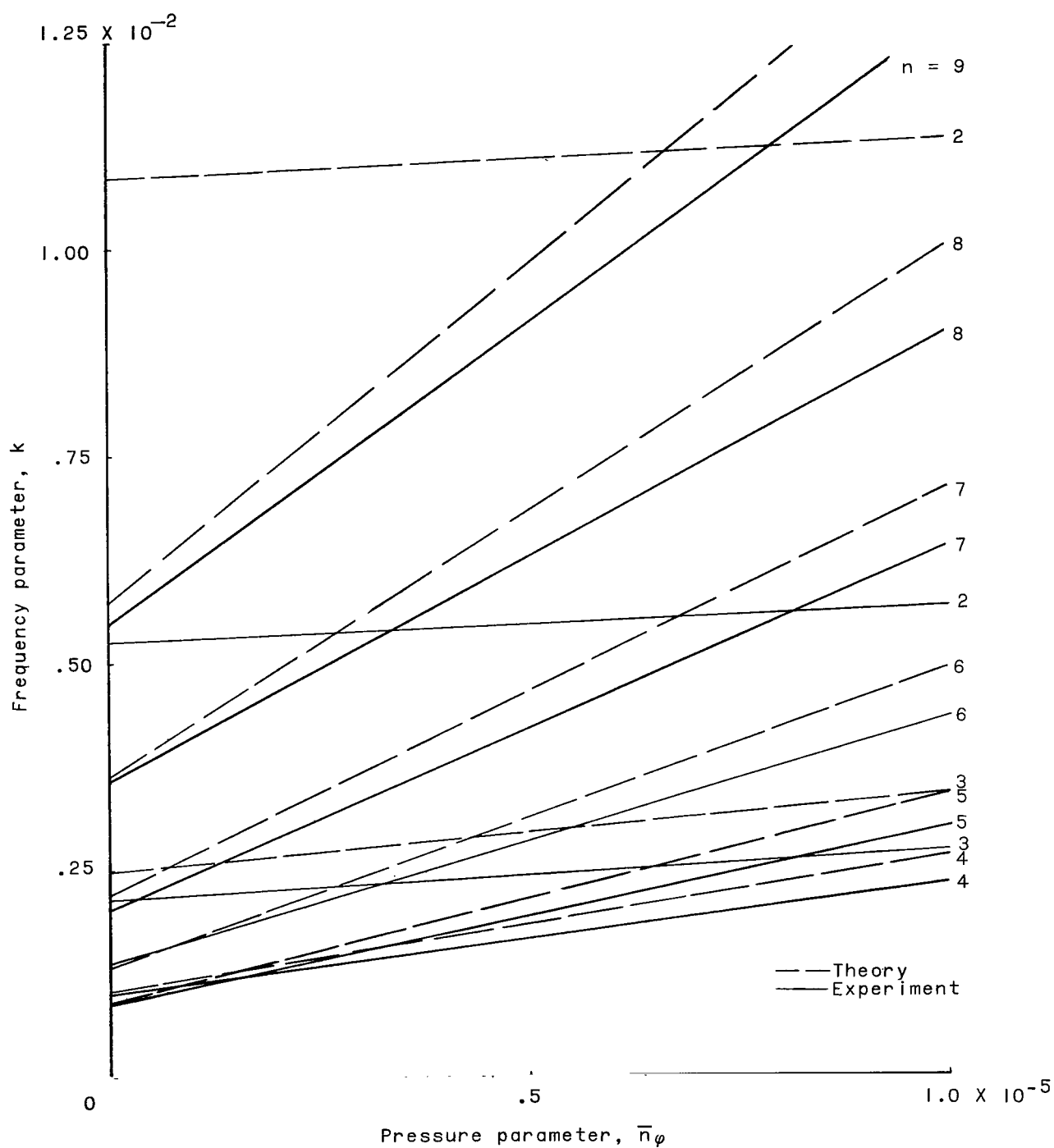


Figure 7.- Variation of frequency and pressure parameter with mode for cylinder 324.  $n_x = 0$ ;  $m = 1$ .

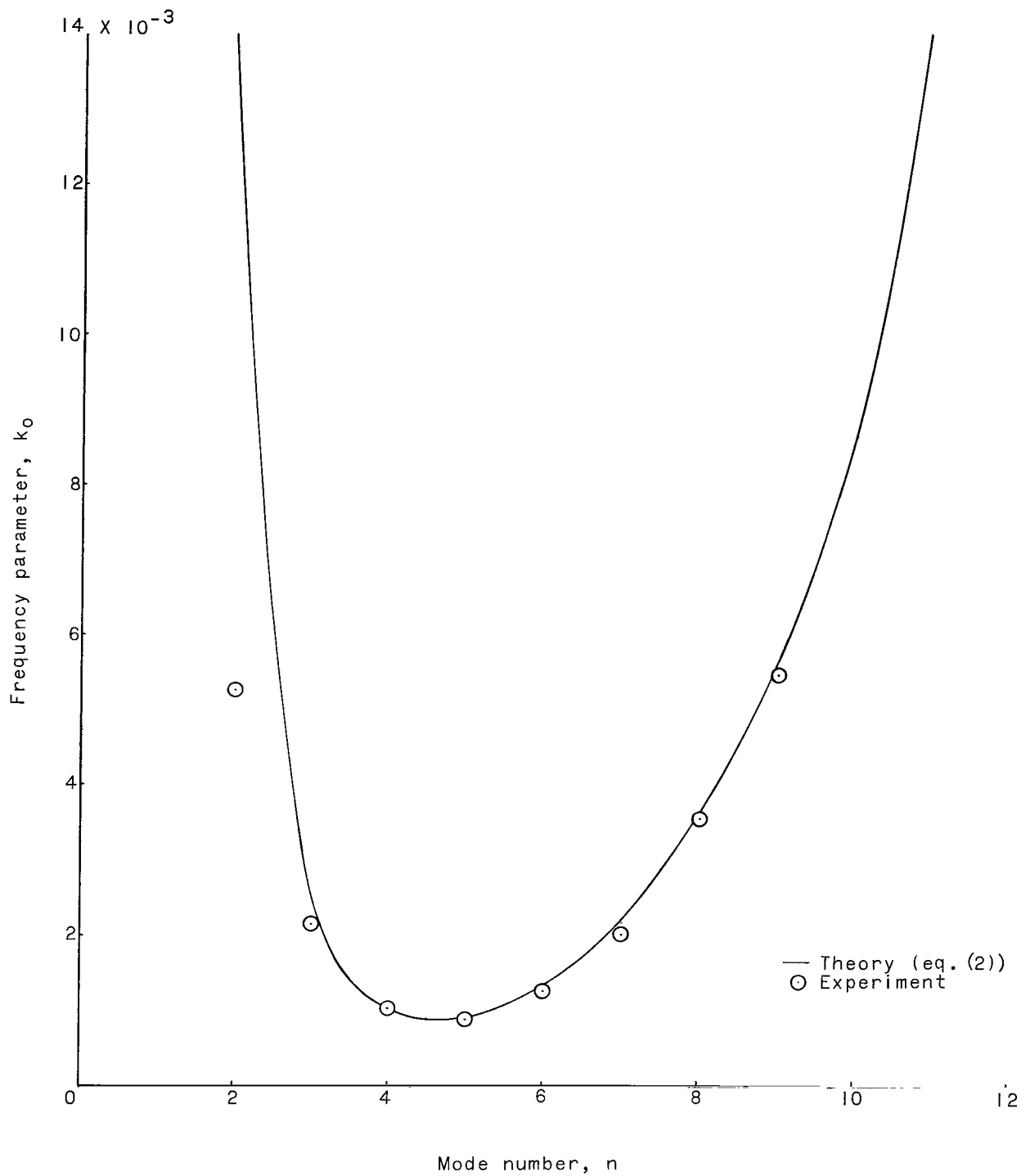


Figure 8.- Experimental and theoretical frequency parameter at zero load for various mode shapes for cylinder 324.  $m = 1$ .



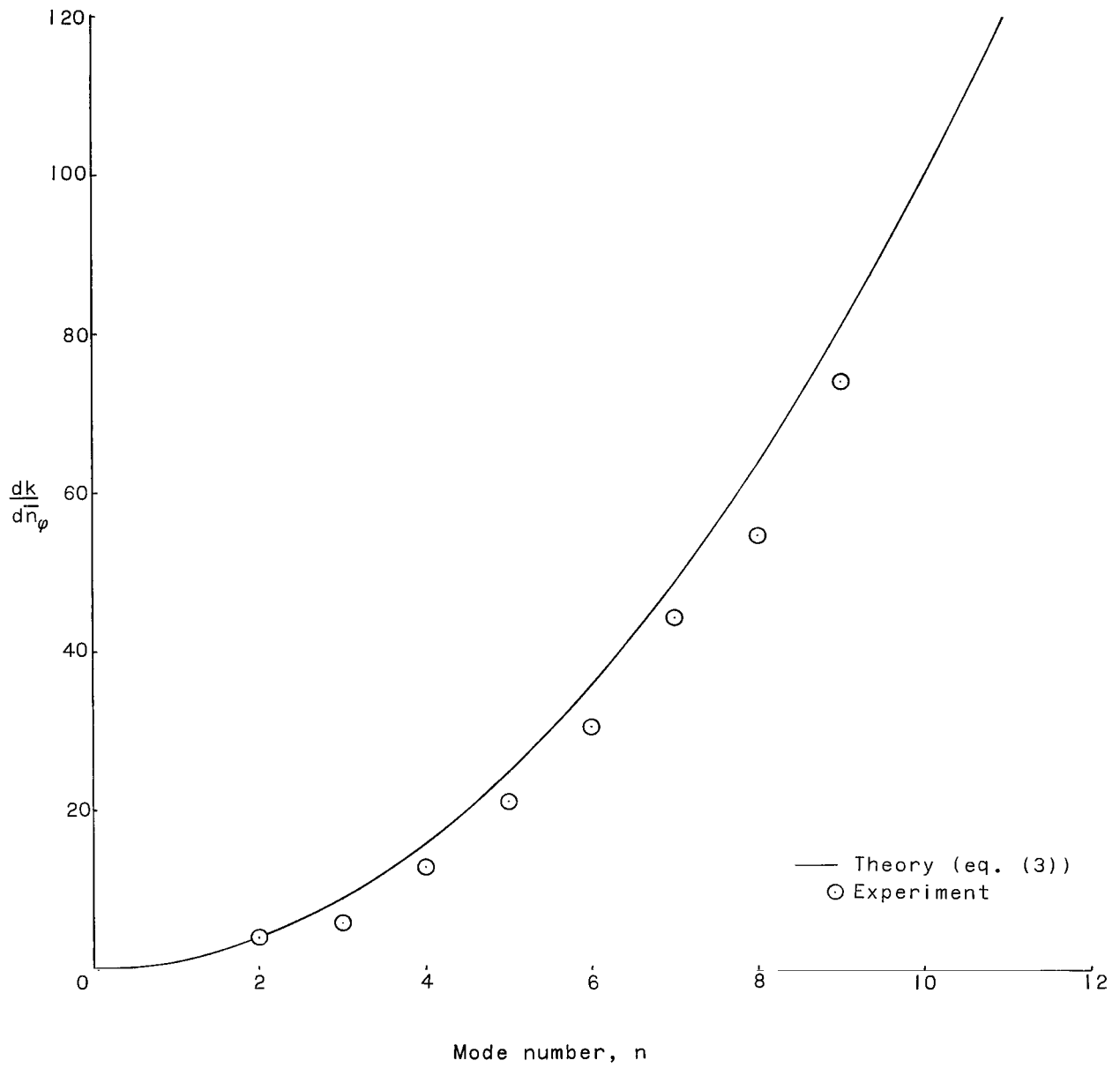
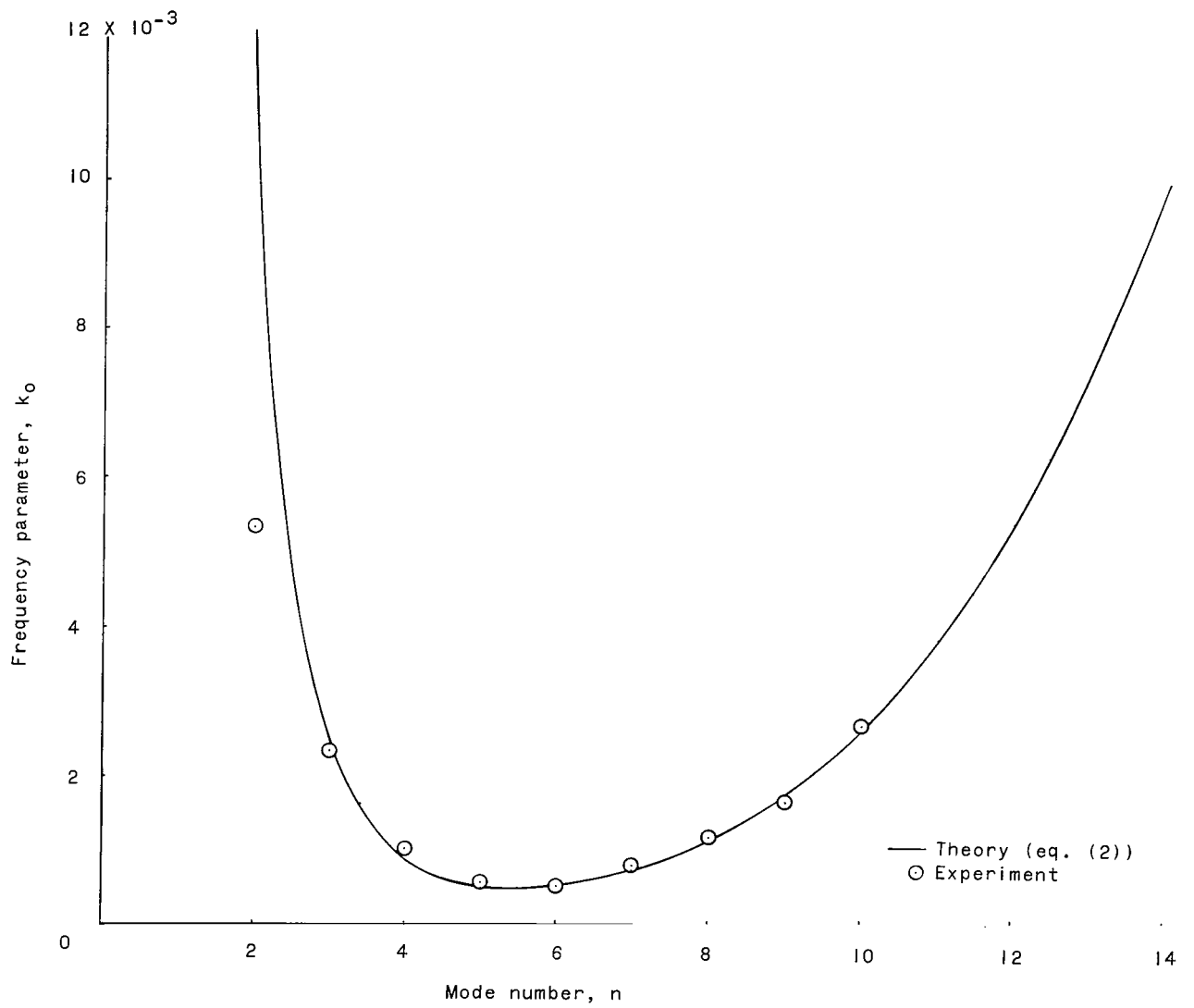
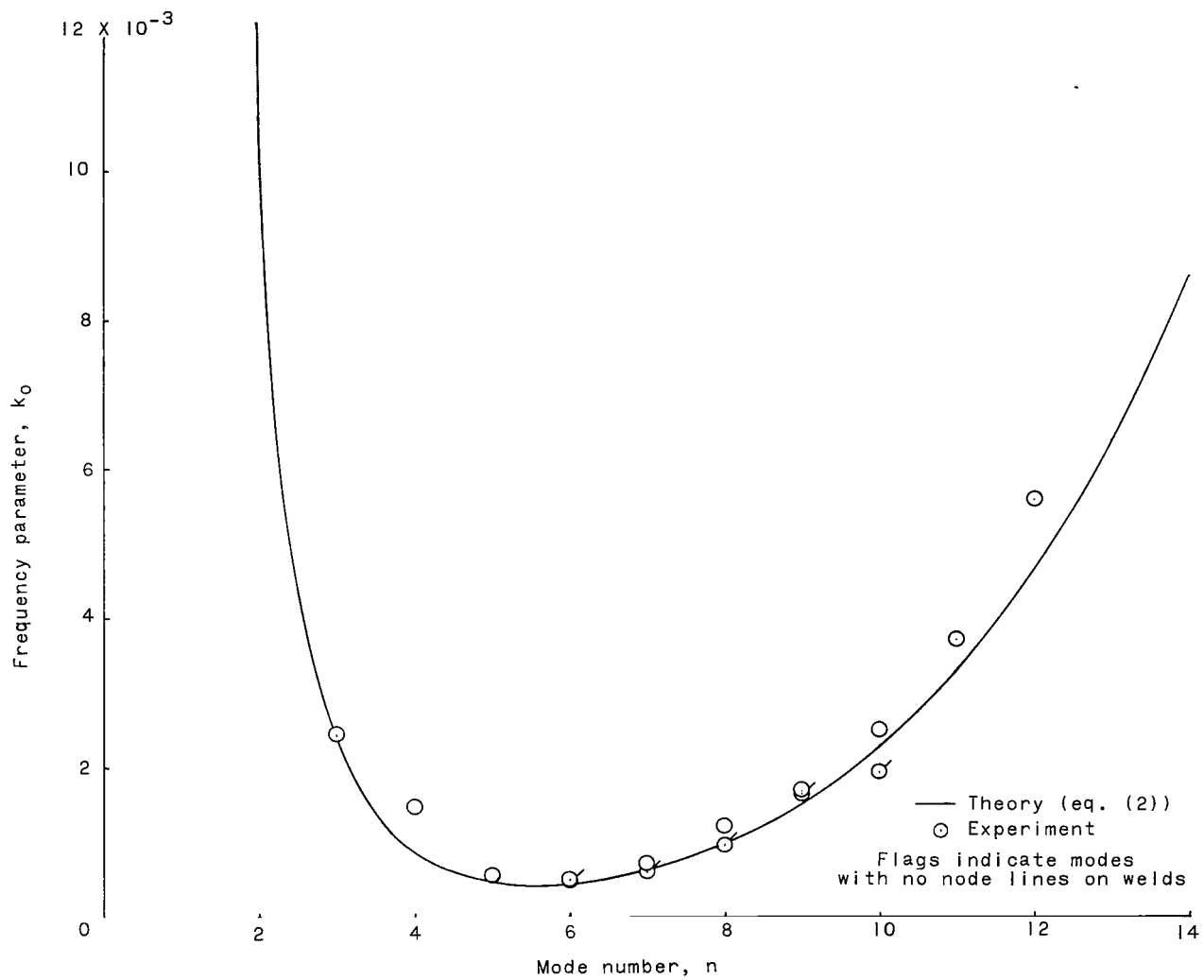


Figure 9.- Experimental and theoretical slope for various mode shapes for cylinder 324.  $m = 1$ .



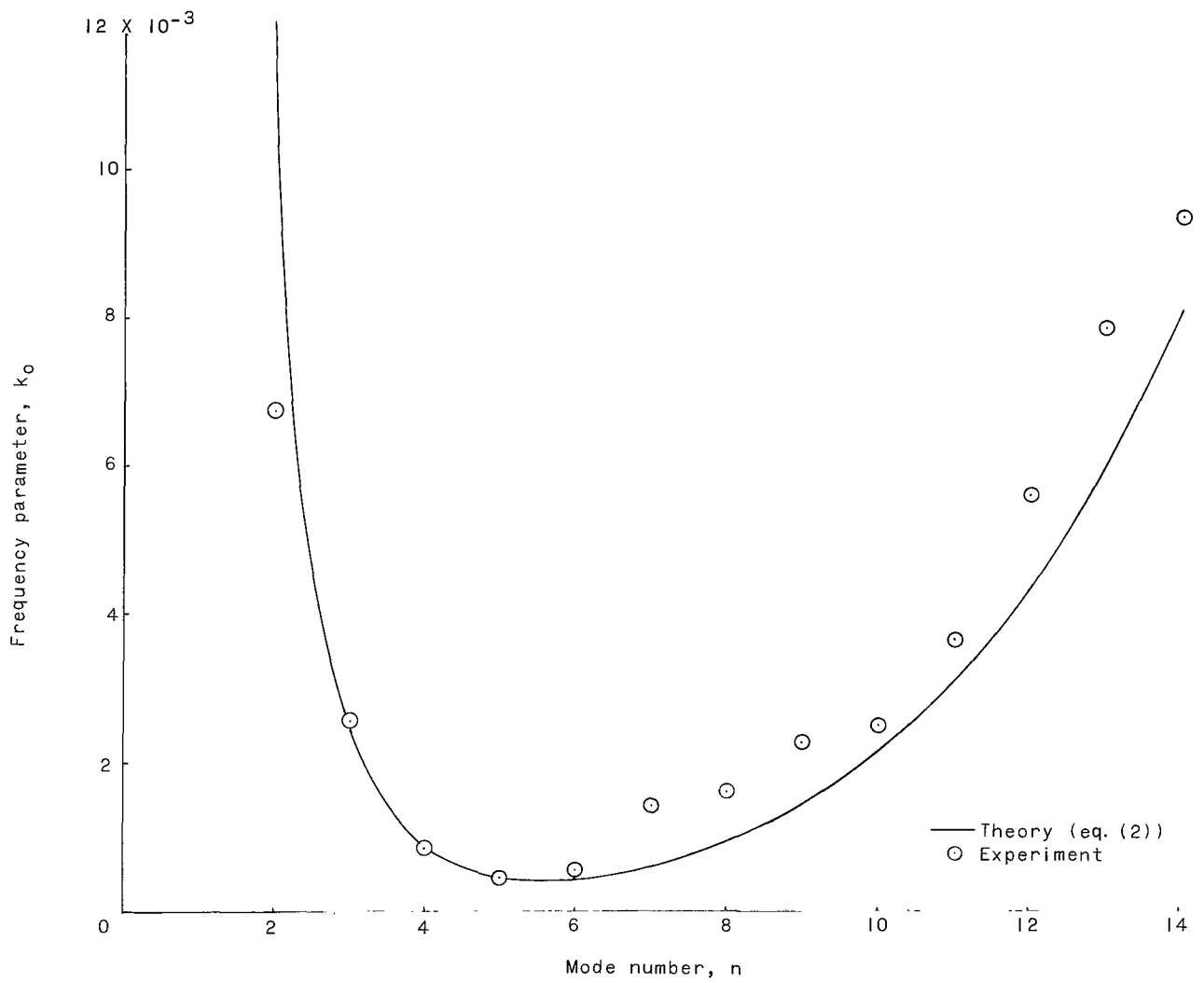
(a) Cylinder 601.

Figure 10.- Experimental and theoretical frequency parameter at zero load for various modes of each cylinder.  $m = 1$ .



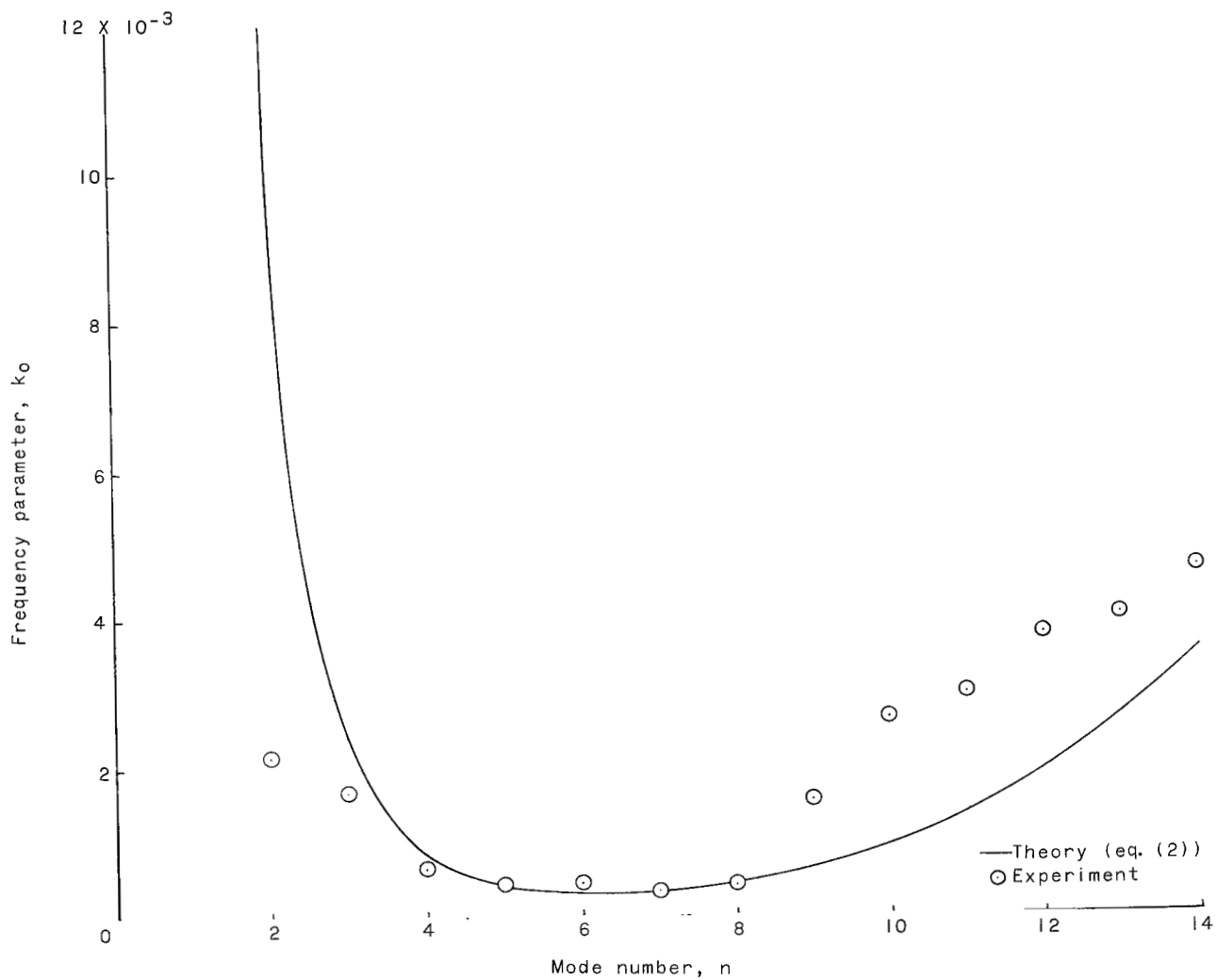
(b) Cylinder 645.

Figure 10.- Continued.



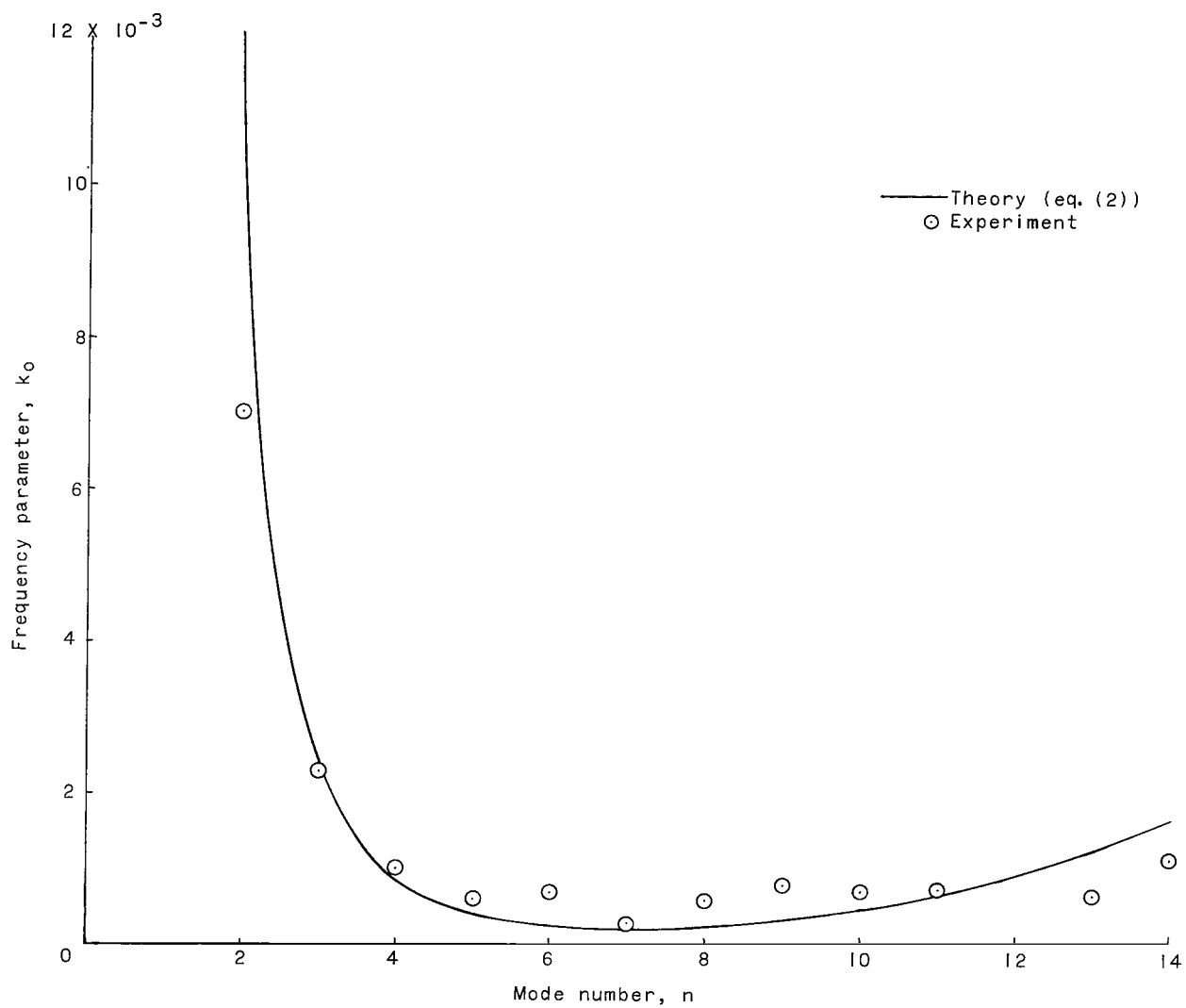
(c) Cylinder 666.

Figure 10.- Continued.



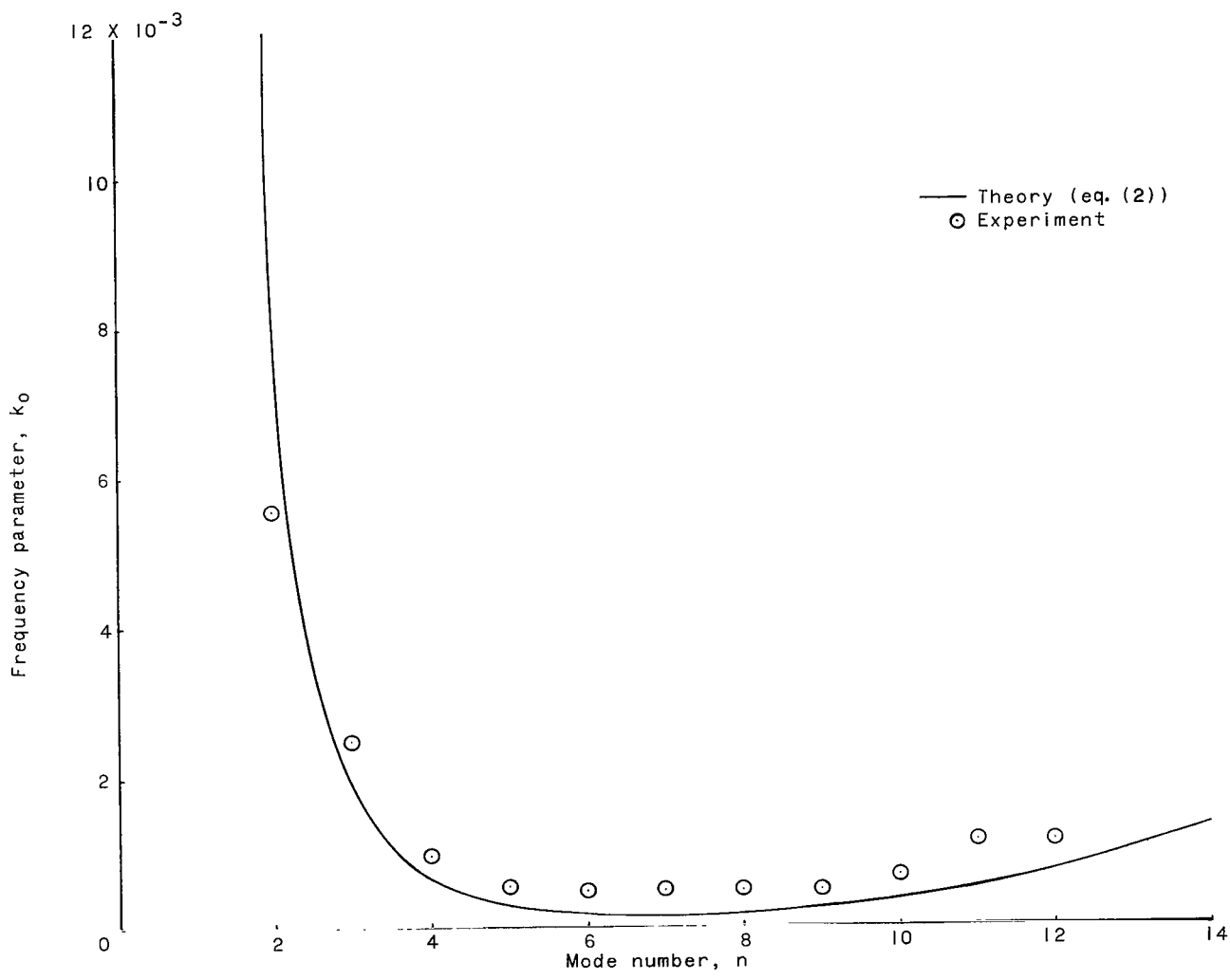
(d) Cylinder 1001.

Figure 10.- Continued.



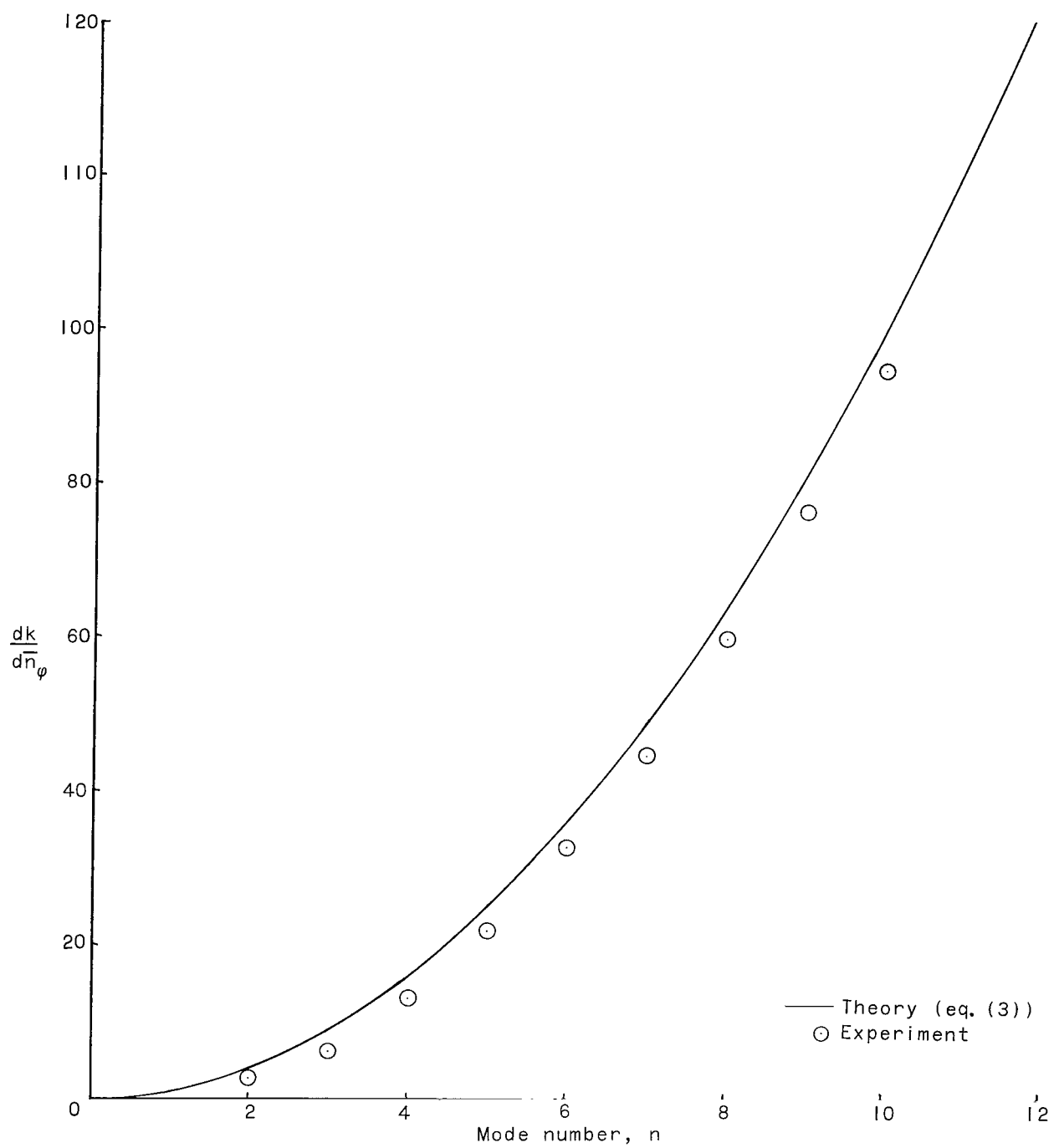
(e) Cylinder 1502.

Figure 10.- Continued.



(f) Cylinder 1624.

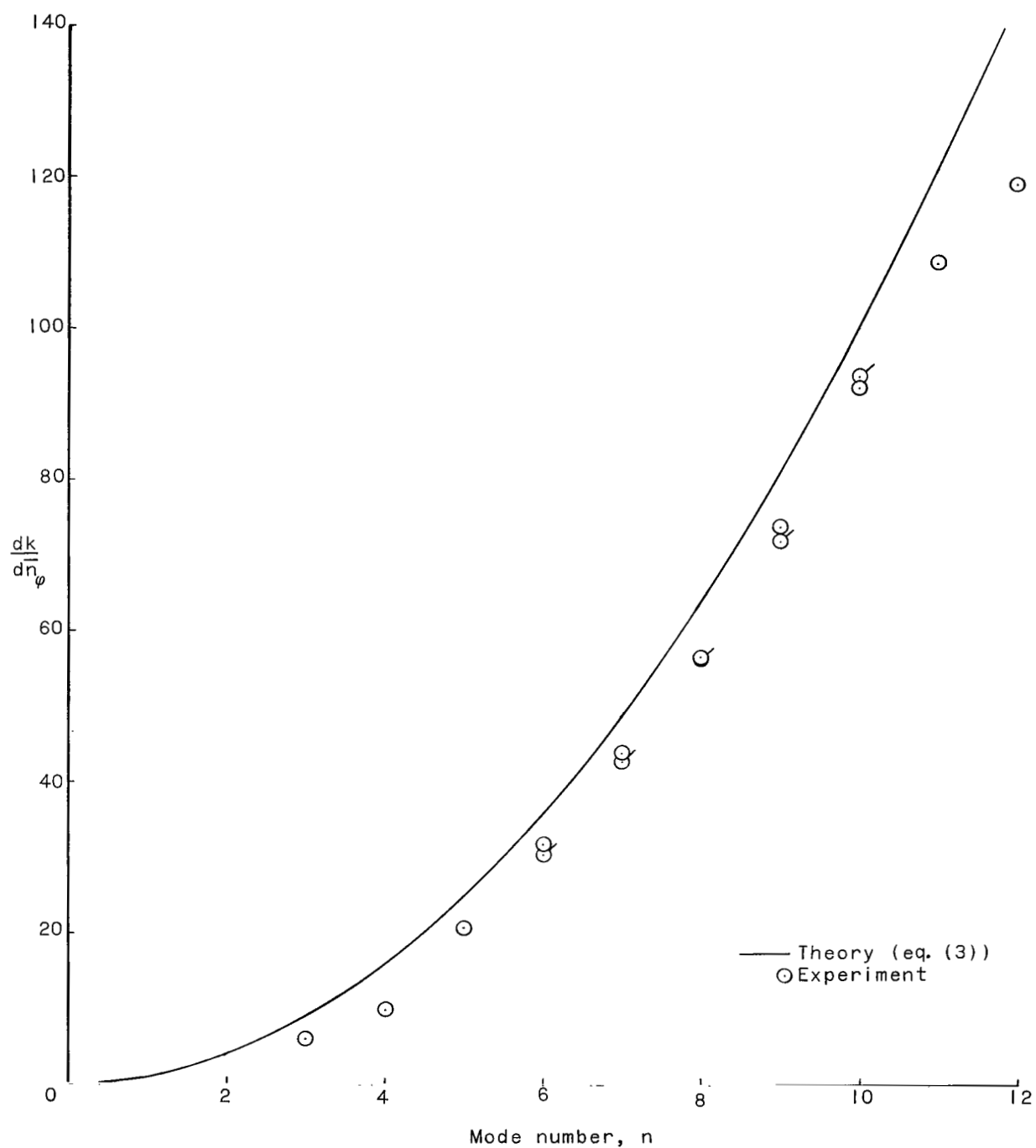
Figure 10.- Concluded.



(a) Cylinder 601.

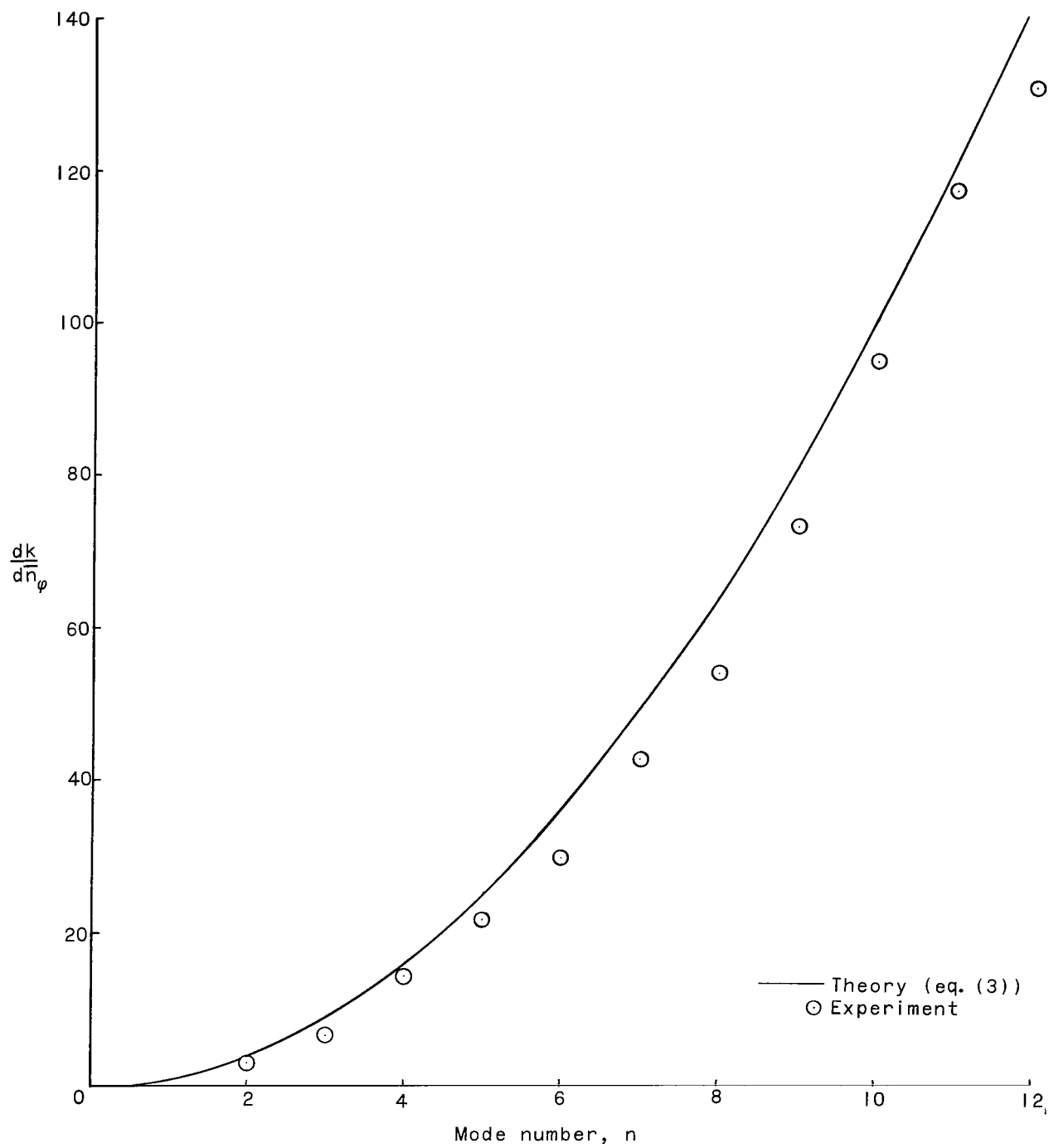
Figure 11.- Experimental and theoretical slope for various modes and cylinders.  $m = 1$ .





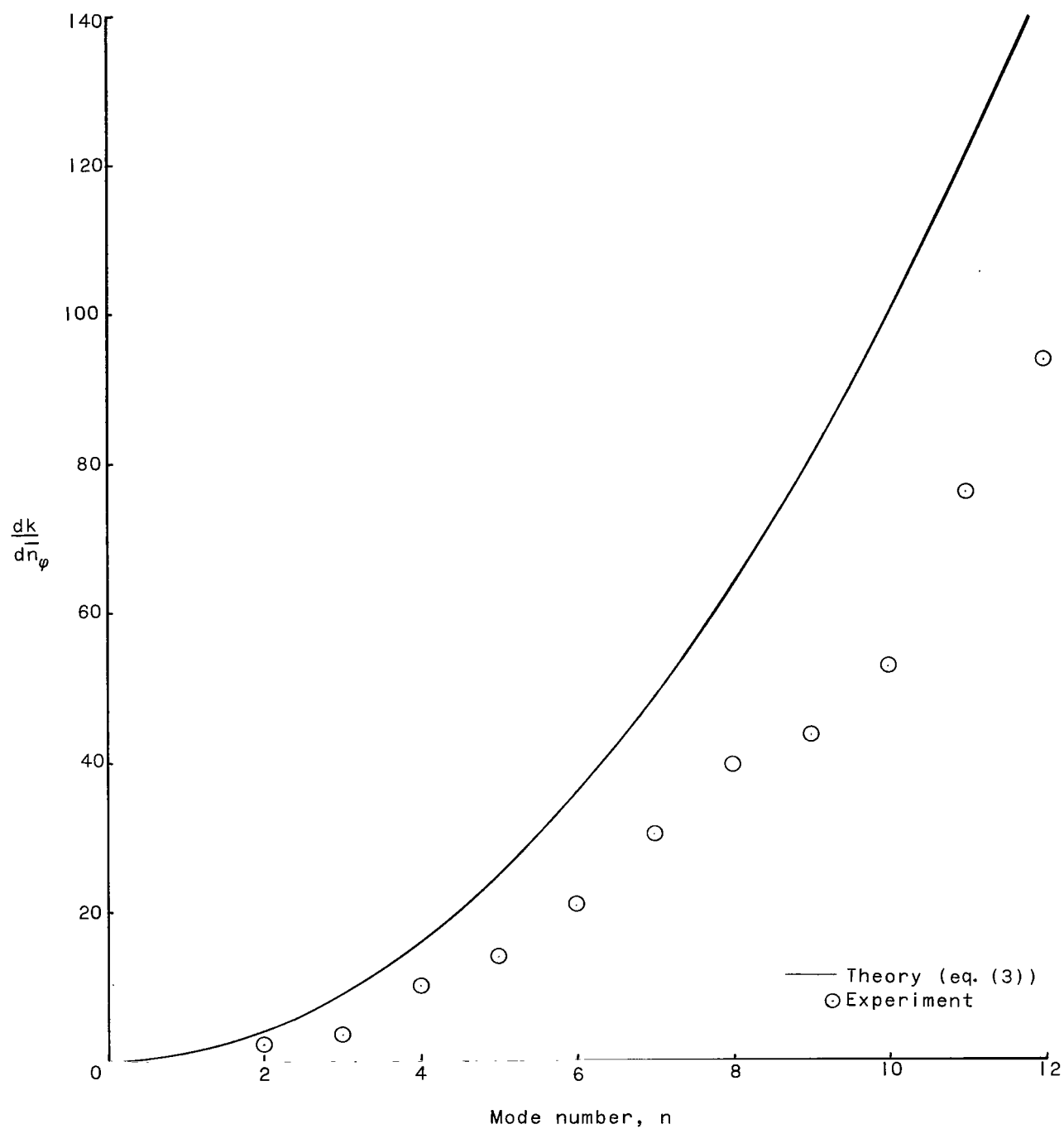
(b) Cylinder 645. Flags indicate modes with no node lines on welds.

Figure 11.- Continued.



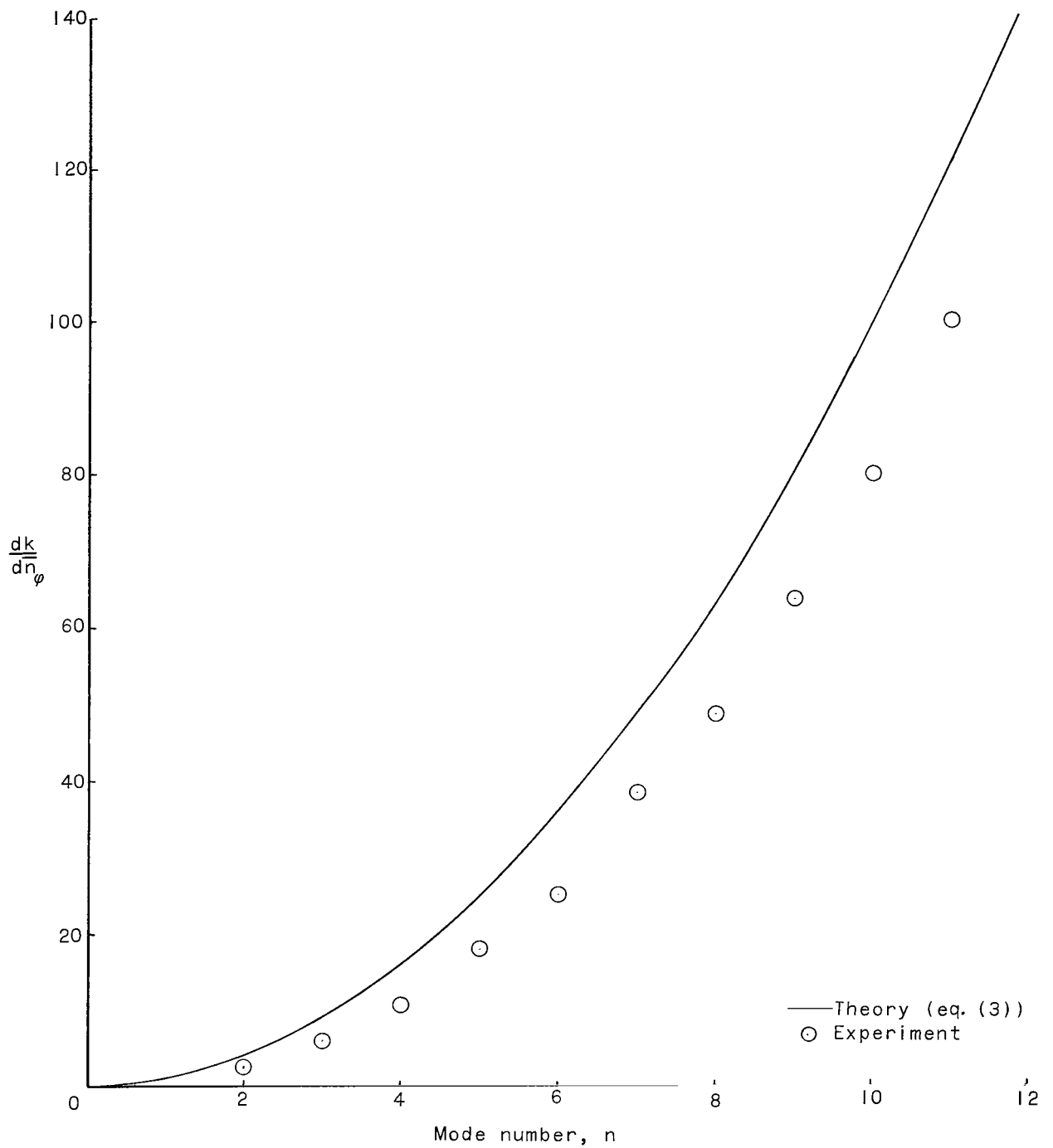
(c) Cylinder 666.

Figure 11.- Continued.



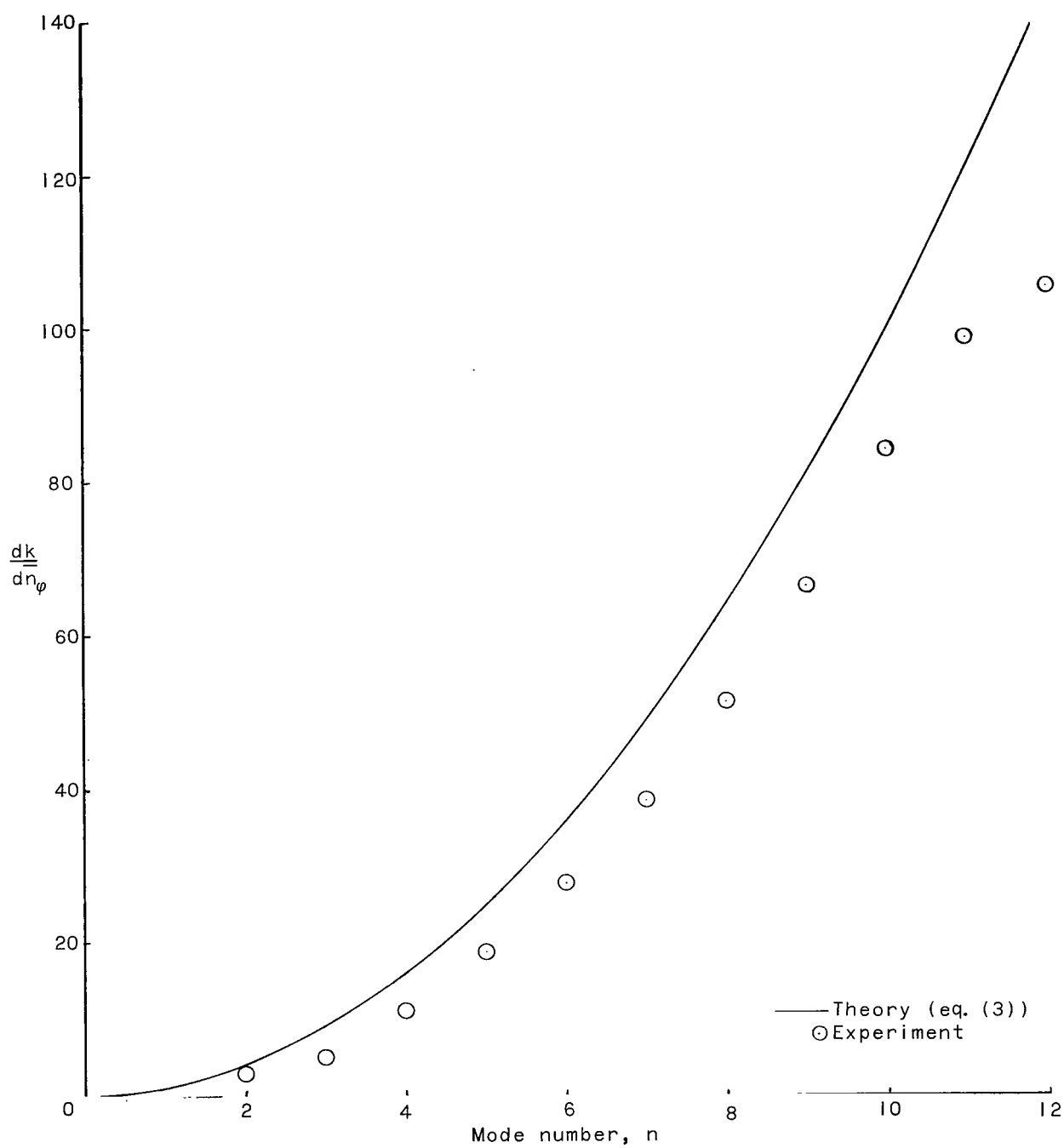
(d) Cylinder 1001.

Figure 11.- Continued.



(e) Cylinder 1502.

Figure 11.- Continued.



(f) Cylinder 1624.

Figure 11.- Concluded.

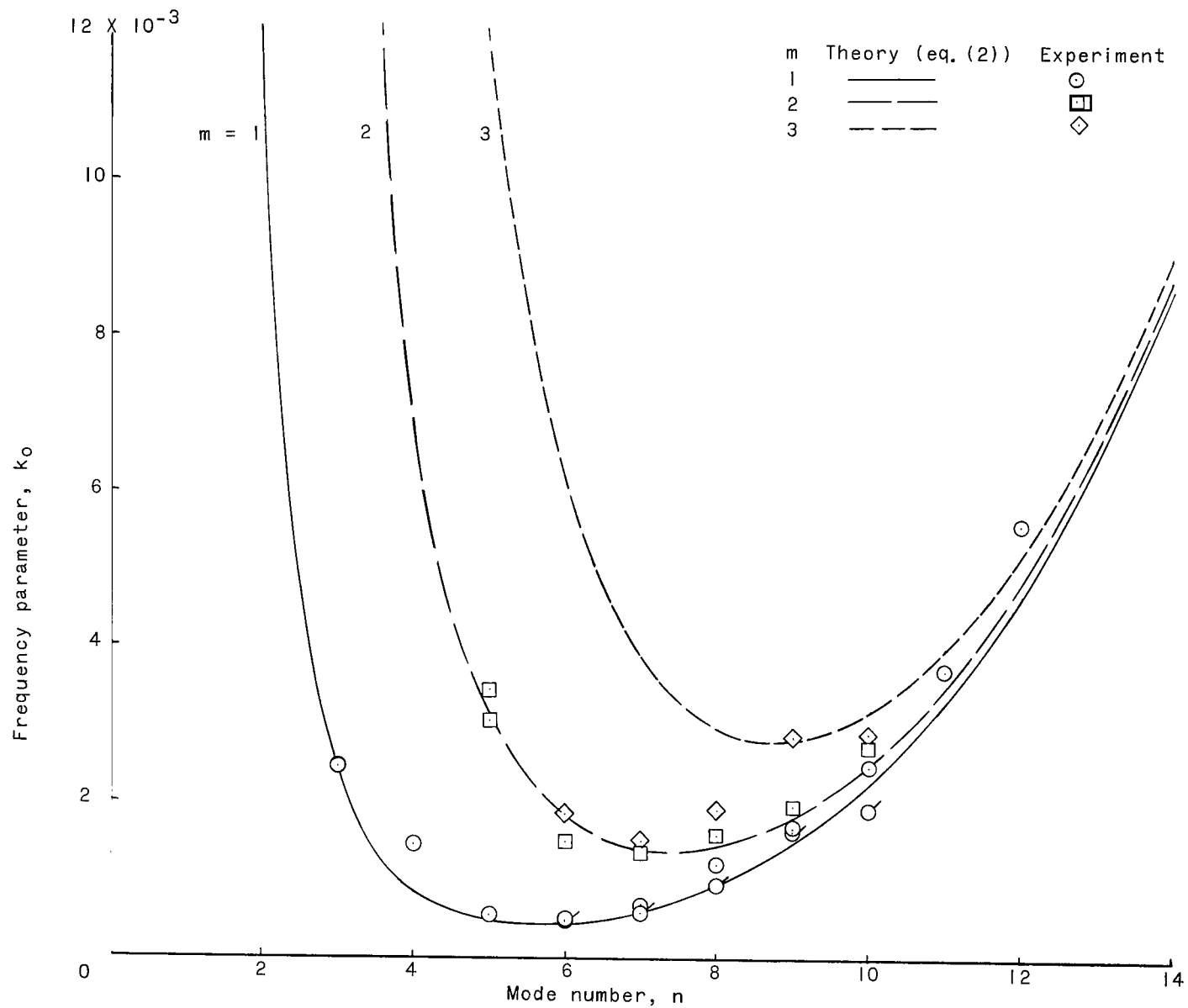


Figure 12.- Experimental and theoretical frequency parameter at zero load for various modes with different longitudinal wave numbers for cylinder 645. Flags indicate modes with no node lines on welds.

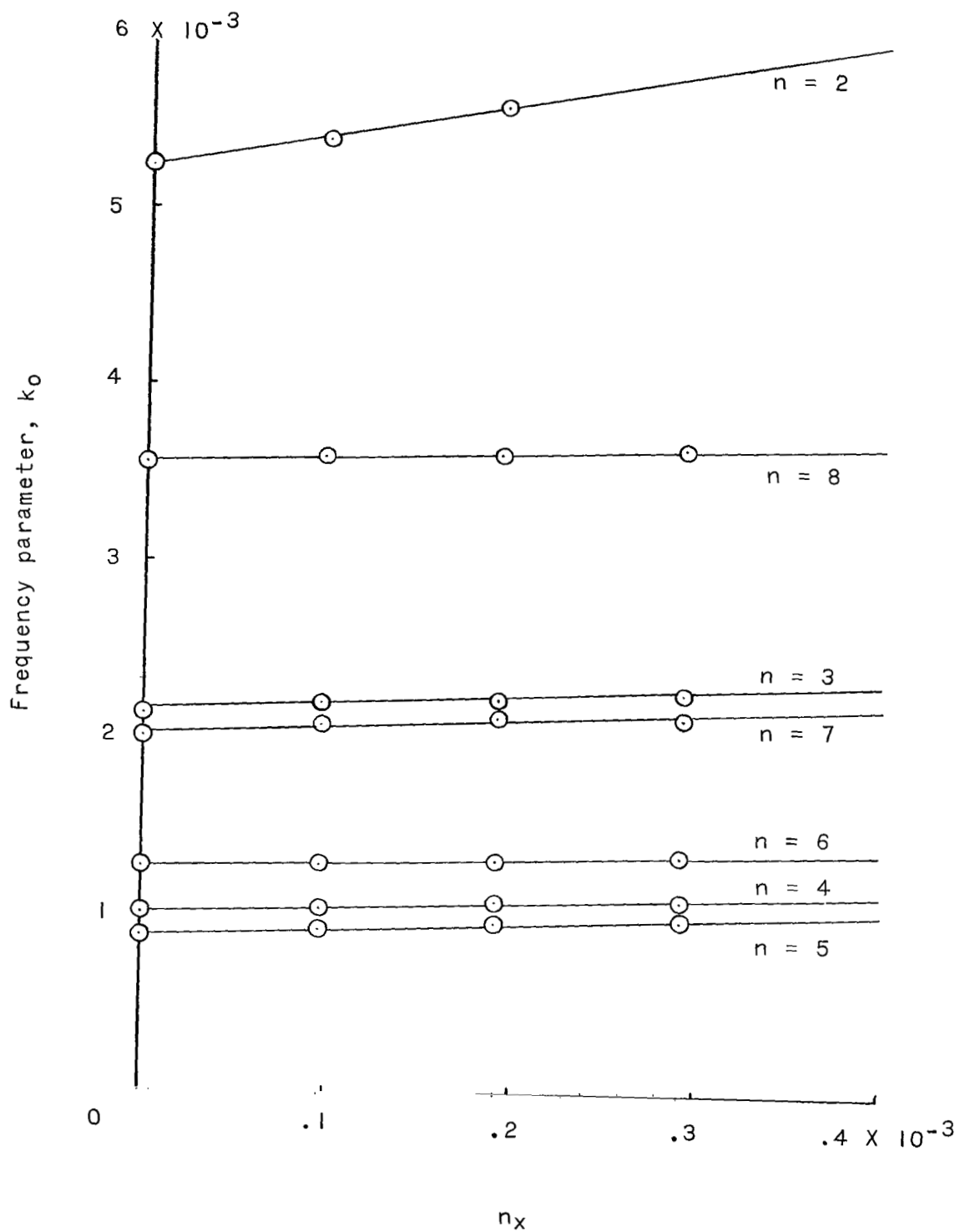


Figure 13.- Experimental variation of frequency parameter due to applied tension for cylinder 324.  $\bar{n}_\varphi = \bar{n}_x = 0$ ;  $m = 1$ .

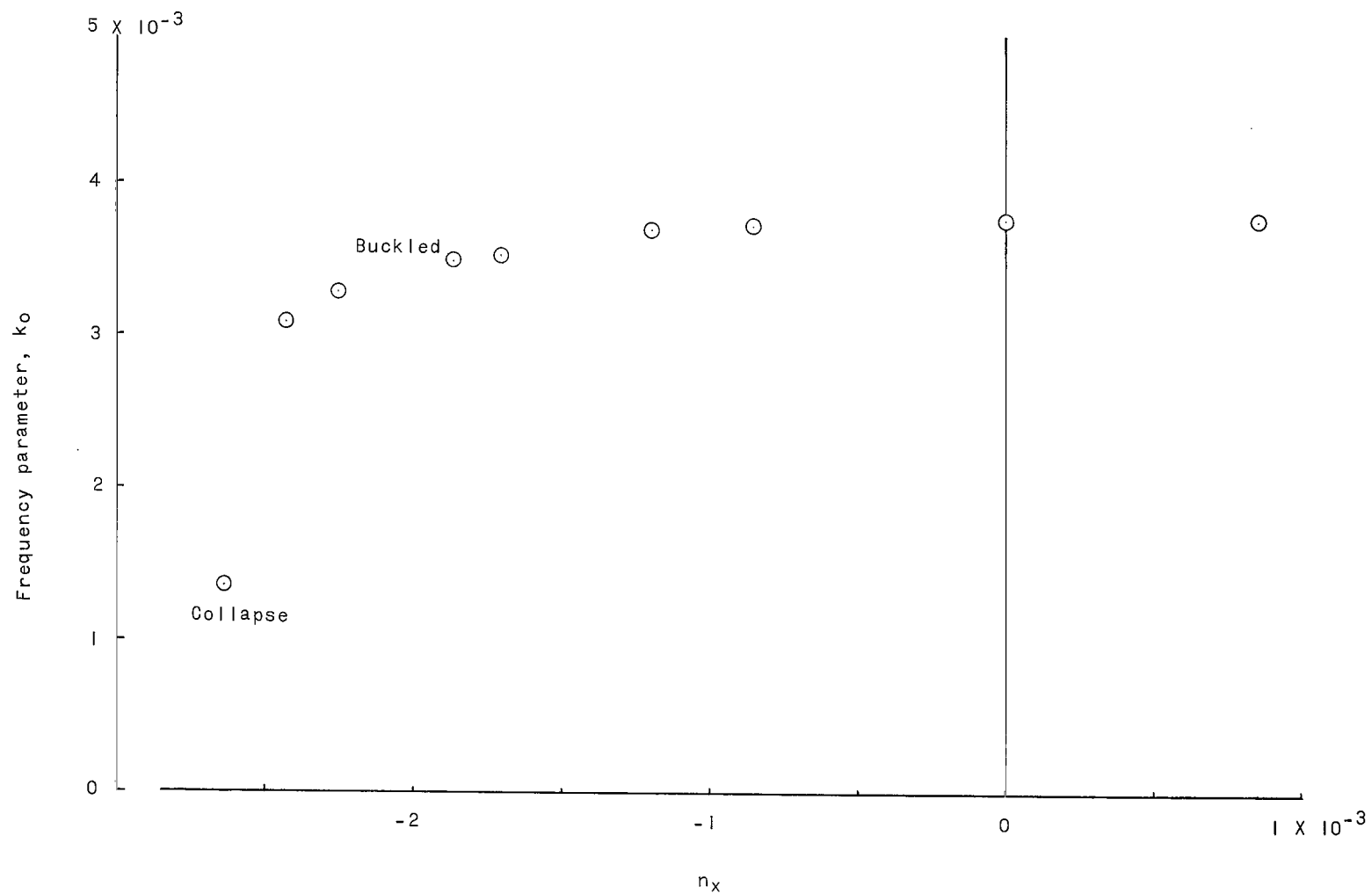


Figure 14.- Experimental frequency variation for mode  $m = 1$ ,  $n = 3$  through the buckling region for cylinder 666.  $\bar{n}_\varphi = 1.8 \times 10^{-6}$ .



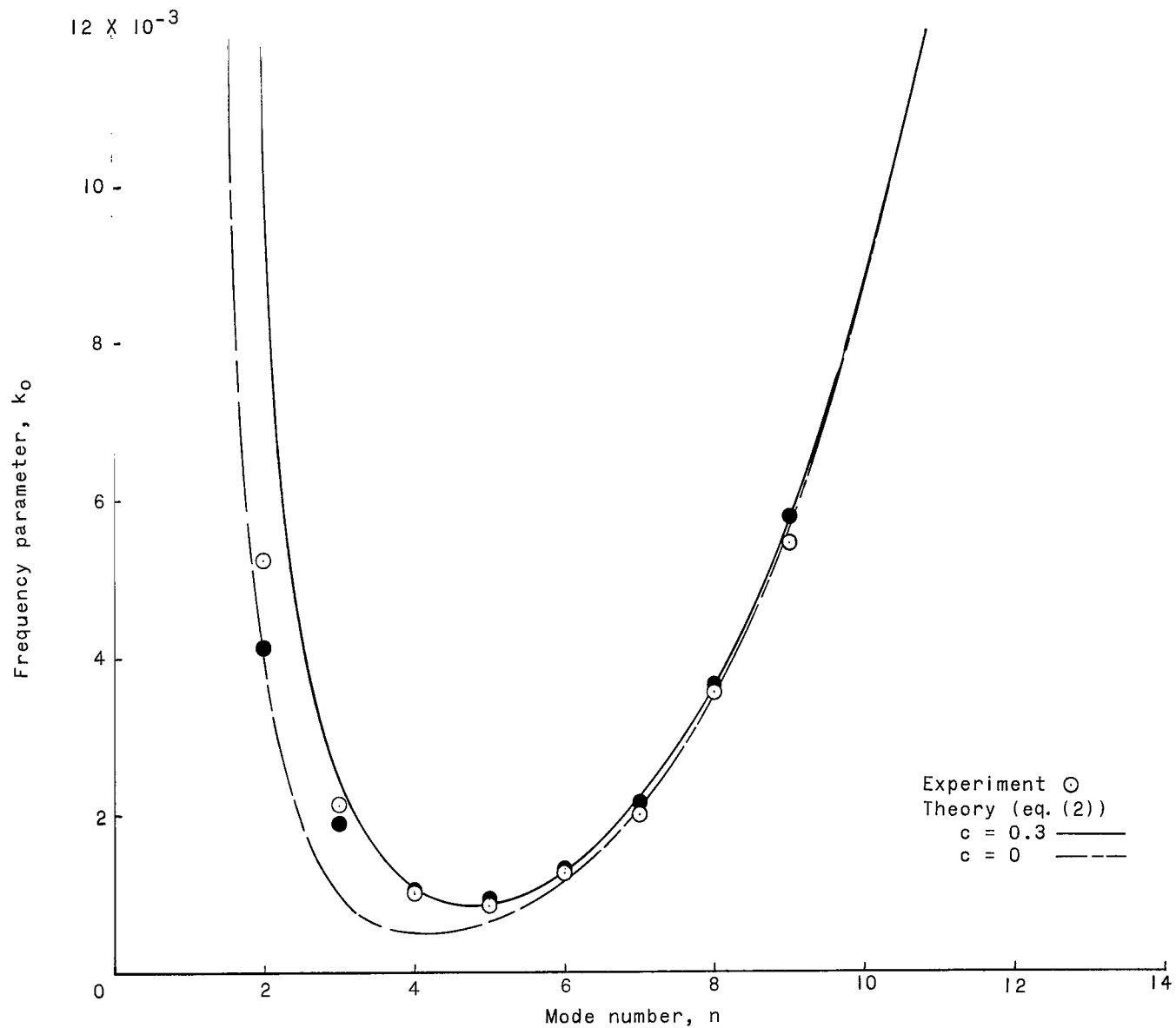


Figure 15.- Experimental and theoretical frequency parameter at zero load for various mode shapes including end fixity for cylinder 324.  $n_x = 0$ ;  $m = 1$ . Dark symbols indicate that the aft ring was free.

3/18/85  
J

*"The aeronautical and space activities of the United States shall be conducted so as to contribute . . . to the expansion of human knowledge of phenomena in the atmosphere and space. The Administration shall provide for the widest practicable and appropriate dissemination of information concerning its activities and the results thereof."*

—NATIONAL AERONAUTICS AND SPACE ACT OF 1958

## NASA SCIENTIFIC AND TECHNICAL PUBLICATIONS

**TECHNICAL REPORTS:** Scientific and technical information considered important, complete, and a lasting contribution to existing knowledge.

**TECHNICAL NOTES:** Information less broad in scope but nevertheless of importance as a contribution to existing knowledge.

**TECHNICAL MEMORANDUMS:** Information receiving limited distribution because of preliminary data, security classification, or other reasons.

**CONTRACTOR REPORTS:** Technical information generated in connection with a NASA contract or grant and released under NASA auspices.

**TECHNICAL TRANSLATIONS:** Information published in a foreign language considered to merit NASA distribution in English.

**TECHNICAL REPRINTS:** Information derived from NASA activities and initially published in the form of journal articles.

**SPECIAL PUBLICATIONS:** Information derived from or of value to NASA activities but not necessarily reporting the results of individual NASA-programmed scientific efforts. Publications include conference proceedings, monographs, data compilations, handbooks, sourcebooks, and special bibliographies.

*Details on the availability of these publications may be obtained from:*

SCIENTIFIC AND TECHNICAL INFORMATION DIVISION  
NATIONAL AERONAUTICS AND SPACE ADMINISTRATION

Washington, D.C. 20546